IEEE Access
Multidisciplinary | Rapid Review | Open Access Journal

Received July 17, 2019, accepted July 19, 2019, date of publication July 23, 2019, date of current version August 8, 2019.

Digital Object Identifier 10.1109/ACCESS.2019.2930658

Prescribed Performance Fault Tolerant Control for Hypersonic Flight Vehicles With Actuator Failures

SIYUAN ZHAO[1] AND XIAOBING LI[2]
[1]Graduate College, Air Force Engineering University, Xi'an 710051, China
[2]Air and Missile Defence College, Air Force Engineering University, Xi'an 710051, China

Corresponding author: Siyuan Zhao (1098547574@qq.com)

This work was supported in part by the National Natural Science Foundation of China under Grant 61603410, Grant 61703424, and Grant 61873278, in part by the Young Talent Fund of University Association for Science and Technology in Shaanxi, China, under Grant 20170107, and in part by the Natural Science Basic Research Plan in Shaanxi Province of China under Grant 2018JQ6024.

ABSTRACT This paper proposes a novel prescribed performance fault tolerant control for hypersonic flight vehicle nonaffine models with actuator failures. First, the hypersonic flight vehicle longitudinal model is decomposed into two subsystems: the altitude subsystem and the velocity subsystem, which are expressed in non-affine forms to design the controller. Second, a novel performance function is used to design the backstepping controller, considering the actuator failures of the altitude subsystem. Different from previous studies, the backstepping controller designed in this paper reduces the steps and computational load. For the velocity subsystem, a prescribed performance fault-tolerant control law is also designed for the nonaffine velocity subsystem with actuator failures. The novel performance function not only guarantees the transient performance and steady-state accuracy of the system but also greatly reduces the overshoot of tracking error. Finally, the Lyapunov functional is used to prove the stability of the designed control system, and the effectiveness and superiority of the method are verified by simulation.

INDEX TERMS Hypersonic flight vehicles, prescribed performance, actuator failures, nonaffine model, backstepping control.

I. INTRODUCTION

After the successful flight test of X-43A and X-51A powered by scramjet engines at the NASA Center in the United States, hypersonic flight vehicle (HFV) has been considered as the most threatening and most trustworthy aircraft in the 21st century [1]–[5]. In principle, HFV can now fly as the speed of ballistic missiles in the atmosphere, but unlike the latter, the trajectory of HFV is complex and difficult to predict [6]–[7]. The development of HFV is a sophisticated, multi-disciplinary and complex project, which combines basic research with engineering test. It involves hypersonic aerodynamics, scramjet technology, new composite materials and thermal protection technology, control technology and integrated technology [8]–[10].

Due to its tightly integrated plane structure, complex and variable flight environment, the HFV dynamic model has the characteristics of uncertainty, nonlinearity, nonaffine and strong coupling, which poses a huge challenge to the design of control system [11], [12]. The advanced aircraft design method enables HFV to possess many undesirable complex dynamic characteristics such as the design of flat and slender fuselage and the use of a large number of light flexible materials increase the flexibility of HFV, which makes it easy to excite flexible modes and cause undesirable body vibration in high-speed flight [13], [14]. The integrated configuration of HFV fuselage engine also requires super-combustible impact. Integrating pressure engine and fuselage make the engine located at the bottom of HFV fuselage produces an additional lift moment while generating thrust, which increases the burden of HFV actuator in starting control to a certain extent. Furthermore, the complex and changeable external environment disturbance and high dynamic pressure caused by high speed in large airspace flight make the actuator very easy to appear failures which lead to stricter control constraints for HFV. Meanwhile, due to the hypersonic flight mission, HFV's control system needs to have satisfactory transient performance and less computational load [15]–[17].

The associate editor coordinating the review of this manuscript and approving it for publication was Chaoyong Li.

In recent ten years, flight control research of HFV emerges in endlessly [18]–[22]. By combining terminal sliding mode control and second-order sliding mode control approach, the second order terminal sliding control is proposed for the velocity and altitude tracking control of the HFV, but it is difficult to ensure the convergence of the system while introducing disturbance [23]. An anti-disturbance backstepping control approach with extended state observer is proposed for tracking control of HFV which considers the large uncertainties, the external disturbances and especially the lack of aerodynamic knowledge, but the boundedness of the tracking error is not explained [24]. Although some achievements have been made in the above research, the actuator mechanism damage and aerodynamic parameters uncertainty of HFV under input saturation state have not been considered. Meanwhile, most of the above researches adopt rigid body model of HFV. Therefore, in order to reduce the crash disaster caused by actuator failures, realize its safe flight and effectively complete the established tasks, it is of great significance to strengthen the research of fault-tolerant control of HFV flexible model [25], [26]. An adaptive fault-tolerant compensation controller with ''switching change'' is designed for HFV with damage faults, but the design process of controller is complex, and the calculation is large [27]. When there are both failures and input saturation problems, a fault-tolerant control method of HFV is designed by reconstructing a new feasible trajectory and transforming saturation into input constraints based on predictive control theory [28].

Most of the existing research results of HFV tracking control are focused on the accuracy of tracking error but ignore the transient performance of the system [29], [30]. A novel constraint approaches variable is used to construct virtual control that guarantees the tracking error within the transient and steady-state performance envelopment [31]. Wei *et al.* study a new adaptive attitude control method which is suitable for target combination of post-capture space robots with unknown inertia and external disturbance to achieve prescribed performance [32]. In order to solve the mismatched uncertainties and differential explosion problems as well as guarantee the steady and transient performance of the tracking error of the original system, Song *et al.* propose a robust dynamic surface controller with given performance for a class of nonlinear feedback systems [33]. Based on these, the prescribed performance control method has been applied to the tracking control of HFV [34], [35]. Zhao et al. study the control design of HFV system with unknown direction control and introduce the fully tuned dynamic radial basis function (RBF) neural network to approximate the unknown term, but the control method is complex form and poor adaptive adjustment ability of parameters [36].

Despite the above research results on HFV flight control, further research has not stopped. Most of the existing studies have not considered the nonaffine control problem of HFV with actuator failures. In fact, for the HFV control inputs, the controller designed for it should be nonaffine one [37], [38]. In this paper, considering the actuator failures, a novel prescribed performance fault tolerant control for HFV nonaffine model is proposed. Firstly, the HFV model is decomposed into subsystems of altitude and velocity which are expressed as nonaffine forms to design controllers respectively. Second, on the basis of considering the actuator failures of the altitude subsystem, a novel prescribed performance function is used to design the backstepping controller. Unlike previous studies, the backstepping controller designed in this paper reduces the steps and computational load. For the velocity subsystem, a prescribed performance fault-tolerant control law is also designed for the nonaffine velocity subsystem with actuator failures. The use of the novel prescribed performance function not only ensures the transient performance and steady-state accuracy, but also reduces the overshoot of tracking error greatly. Finally, Lyapunov functional is used to prove the stability of the designed control system, and the effectiveness and superiority of the proposed method are verified by contrast simulation. The main contributions of this paper are summarized as follows:

1. The control method designed in this paper is based on the nonaffine models of HFV, which are closer to the actual flight situation than previous studies. The novel prescribed performance function is introduced to ensure the transient performance and steady-state accuracy of small overshoot control system.

2. Considering the actuator failures of HFV altitude and velocity subsystem, the failure model is also considered as a nonaffine model. RBF neural network is introduced to approximate the fault term which simplifies the controller design.

3. The uncertainties in HFV flight control are realized by using backstepping control method to meet the requirements of matching conditions. There are less steps in backstepping design and low computational load.

4. In order to verify the robustness of the system, perturbations are added to the aerodynamic parameters. Compared with existing three control methods, the control method proposed in this paper has better tracking performance and robustness. Meanwhile, the HFV model initial value is changed and simulated again. From the simulation results, the method presented in this paper has certain effectiveness.

The rest of this paper is outlined as follows. Section 2 introduces the motion model of HFV and the novel prescribed performance function. Section 3 studies the controller and proves its stability. The contrast simulation results are presented in Section 4. The final conclusion is proposed in Section 5.

II. MODEL DESCRIPTION AND PRELIMINARIES

A. HFV DYNAMICS MODEL AND PRELIMINARIES

In this paper, the control-oriented nonlinear model of HFV from Parker [37-38] is adopted, and its longitudinal plane stress is shown in Fig. 1. The longitudinal dynamic model of HFV derived from the standard Lagrange equation can be expressed as follows:

$$\dot{V} = \frac{T\cos\alpha - D}{m} - g\sin\gamma \tag{1}$$

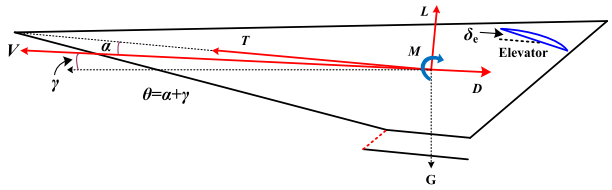

FIGURE 1. Force map of a hypersonic vehicle model.

$$\dot{h} = V\sin\gamma \tag{2}$$

$$\dot{\gamma} = \frac{L + T\sin\alpha}{mV} - \frac{g\cos\gamma}{V} \tag{3}$$

$$\dot{\theta} = Q \tag{4}$$

$$\dot{Q} = \frac{M + \tilde{\psi}_1\ddot{\eta}_1 + \tilde{\psi}_2\ddot{\eta}_2}{I_{yy}} \tag{5}$$

$$\begin{aligned} k_1\ddot{\eta}_1 = &-2\zeta_1\omega_1\dot{\eta}_1 - \omega_1^2\eta_1 + N_1 \\ &- \tilde{\psi}_1\frac{M}{I_{yy}} - \frac{\tilde{\psi}_1\tilde{\psi}_2\ddot{\eta}_2}{I_{yy}} \end{aligned} \tag{6}$$

$$\begin{aligned} k_2\ddot{\eta}_2 = &-2\zeta_2\omega_2\dot{\eta}_2 - \omega_2^2\eta_2 + N_2 \\ &- \tilde{\psi}_2\frac{M}{I_{yy}} - \frac{\tilde{\psi}_2\tilde{\psi}_1\ddot{\eta}_1}{I_{yy}} \end{aligned} \tag{7}$$

The above vehicle model has five rigid body states (velocity V, altitude h, flight path angle γ, pitch angle θ, pitch rate Q) and two flexible states (η_1 and η_2). Moreover, m and I_{yy} denote the mass of HFV and moment of inertia.

The attack angle $\alpha = \theta - \gamma$. L, T, D, M, N_i, ζ_i, ω_i and $\tilde{\psi}_i$ denote lift force, thrust force, drag force, pitching moment, the ith generalized force, damping ratio for flexible state η_i, natural frequency for flexible state η_i and constrained beam coupling constant for flexible state η_i. Their details are as follows:

$$\begin{cases} T \approx [\beta_1(h,\overline{q})\Phi + \beta_2(h,\overline{q})]\alpha^3 \\ \quad + [\beta_3(h,\overline{q})\Phi + \beta_4(h,\overline{q})]\alpha^2 \\ \quad + [\beta_5(h,\overline{q})\Phi + \beta_6(h,\overline{q})]\alpha \\ \quad [\beta_7(h,\overline{q})\Phi + \beta_8(h,\overline{q})] \\ D \approx \overline{q}S\left(C_D^{\alpha^2}\alpha^2 + C_D^{\alpha}\alpha + C_D^{\delta_e^2}\delta_e^2 + C_D^{\delta_e}\delta_e + C_D^0\right) \\ L \approx \overline{q}S\left(C_L^{\alpha}\alpha + C_L^{\delta_e}\delta_e + C_L^0\right) \\ M \approx z_T T + \overline{q}S\overline{c}\left(C_{M,\alpha}^{\alpha^2}\alpha^2 + C_{M,\alpha}^{\alpha}\alpha + C_{M,\alpha}^0 + c_e\delta_e\right) \\ N_1 = N_1^{\alpha^2}\alpha^2 + N_1^{\alpha}\alpha + N_1^0 \\ N_2 = N_2^{\alpha^2}\alpha^2 + N_2^{\alpha}\alpha + N_2^{\delta_e}\delta_e + N_2^0 \\ \overline{q} = \frac{1}{2}\overline{\rho}V^2,\ \overline{\rho} = \overline{\rho}_0\exp[(h_0 - h)/h_s] \end{cases} \tag{8}$$

where $\overline{q}$ is air dynamics pressure, $\overline{\rho}$, S, $\overline{c}$ and z_T denote air density, reference area, aerodynamic chord and thrust arm.

It can be seen from (1)∼(8), the control inputs are fuel-to-air ratio Φ and elevator angular deflection δ_e, and the outputs are velocity V and altitude h. The control goal is to devise non-affine prescribed performance controllers Φ and δ_e via backstepping for HFV such that velocity V and altitude h can track their reference commands V_{ref} and h_{ref} in the presence of parametric uncertainties. It can be seen that the control inputs Φ and δ_e do not occur explicitly in (1)∼(7) but appear through L, T, D, M, N_1 and N_2. For more detailed definitions of other parameters and coefficients, the readers could refer to [38].

Remark 1: Obviously, the flexible states can't be measured for control design. When designing controllers, they are treated as system uncertainties that are coped with by the controller's robustness.

From (1)∼(8), it can be also seen, the flexible states of HFV are coupled with the rigid states severely by aerodynamic force L, T, D, M. If the effect of restraining the flexible states is not obvious, the control of the rigid states will be greatly affected. Therefore, the mission of the control system is not only to ensure the stability of the rigid-body system to track the reference inputs, but also to ensure the ultimate convergence of the flexible states [39].

Assumption 1 (see [40]): The desired reference inputs V_{ref} and h_{ref} are known and bounded, as well as their derivatives.

Lemma 1 (see [41], [42]): For any given continuous function y on a compact set $\Omega_{\mathbf{Z}}$, there is an RBF neural network $\boldsymbol{W}^T S(\mathbf{Z})$, such that

$$y = \boldsymbol{W}^T S(\mathbf{Z}) \tag{9}$$

where $\boldsymbol{W}$ is weight parameter vector and $S(\mathbf{Z})$ is the basis function vector which is expressed as $S(\mathbf{Z}) = \left[s_1(\mathbf{Z}), s_2(\mathbf{Z}), \cdots, s_p(\mathbf{Z})\right]^T$. $s_i(Z)$ is selected as following Gaussian function

$$s_i(\mathbf{Z}) = \exp\left[-\frac{\|\mathbf{Z} - \boldsymbol{a}_i\|^2}{b_i^2}\right], \quad i = 0, 1, \cdots, p \tag{10}$$

where $\boldsymbol{a}_i = [a_1, a_2, \cdots, a_n] \in R^{\mathrm{n}}$ represents the center vector and $b_i \in \mathbf{R}^+$ is the width of the Gaussian function. n and p denote dimension of input vector and number of nodes.

If enough nodes are selected, there must be an ideal weight vector $\boldsymbol{W}^* = \left[w_1^*, w_2^*, \cdots, w_p^*\right]^T \in \mathbf{R}^p$ for any nonlinear continuous function $F(\mathbf{Z})$, such that

$$F(\mathbf{Z}) = \boldsymbol{W}^{\boldsymbol{T}} S(\mathbf{Z}) + \delta \tag{11}$$

where $|\delta| \le \delta_{\mathrm{M}}$ is approximation error, δ_{M} is the upper bound of approximation error.

B. PRESCRIBED PERFORMANCE

Define a continuous function $\vartheta(t)$ that satisfies the following two conditions simultaneously, called performance function [29], [30].

(1) Performance function is continuously differentiable, bounded, strictly positive and decreasing function of time.

(2) $\lim_{t\to\infty} \vartheta(t) = \vartheta_\infty > 0$.

According to the definition of performance function, this paper chooses the following function as the performance function.

$$\begin{cases} \vartheta_l(t) = [\tanh e(t) - 1/2]\,\vartheta(t) - \tanh(e(t))\,\vartheta_\infty \\ \vartheta_r(t) = [\tanh e(t) + 1/2]\,\vartheta(t) - \tanh(e(t))\,\vartheta_\infty \end{cases} \tag{12}$$

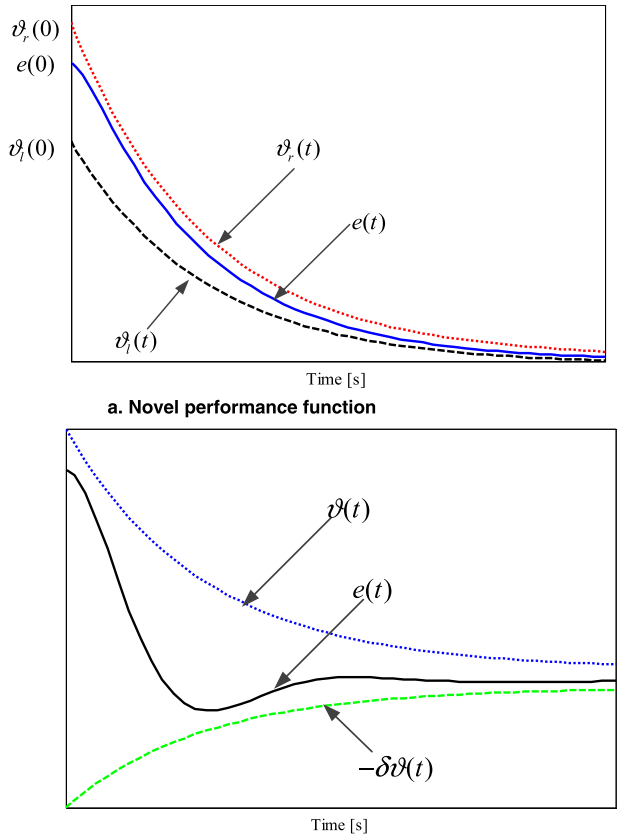

FIGURE 2. Prescribed novel performance function.

where $\vartheta(t) = (\vartheta_0 - \vartheta_\infty) e^{-lt} + \vartheta_\infty$ and $\vartheta_0, \vartheta_\infty, l \in R^+$ are design parameters. l is related to the adjustment time, ϑ_0 and ϑ_∞ are related to overshoot.

Define tracking error $e(t)$ as

$$\vartheta_l(t) < e(t) < \vartheta_r(t) \tag{13}$$

Remark 1: Traditional performance function $\vartheta(t)$ has certain prescribed reliability, but it requires high accuracy of tracking error and does not have small overshoot characteristics [43]. On one hand, the probability of control singularity is reduced, and on the other hand, the overshoot of tracking error is reduced. The following Fig. 2 shows that the novel performance function constructed by introducing hyperbolic tangent function can adaptively change its shape according to the change of tracking error. Furthermore, by reasonably selecting the parameters of the novel performance function, the tracking error can be small overshoot or even zero overshoot.

Since the control law cannot be directly designed via Eq. (13), the transform error function $\varepsilon(t)$ is introduced to transform the constrained system into an unconstrained equivalent system.

$$\varepsilon(t) = \ln\left(\frac{\tau(t)}{1-\tau(t)}\right) \tag{14}$$

with $\tau(t) = [e(t) - \vartheta_l(t)]/[\vartheta_r(t) - \vartheta_l(t)]$.

The time derivative of Eq. (14) is given by

$$\dot{\varepsilon}(t) = r\{\dot{e}(t) + \frac{\vartheta_l(t)\dot{\vartheta}_r(t) - \dot{\vartheta}_l(t)\vartheta_r(t)}{\vartheta_r(t) - \vartheta_l(t)} - \frac{e(t)\left[\dot{\vartheta}_r(t) - \dot{\vartheta}_l(t)\right]}{\vartheta_r(t) - \vartheta_l(t)}\} \tag{15}$$

with $r = \frac{1}{(1-\tau(t))(\vartheta_r(t)-\vartheta_l(t))\tau(t)} > 0$.

Theorem 1: If $\varepsilon(t)$ is bounded, there is $\vartheta_l(t) < e(t) < \vartheta_r(t)$.

Proof: Because $\varepsilon(t)$ is bounded, there is a positive constant ε_M and $|\varepsilon(t)| \le \varepsilon_M$. Moreover, the inverse transformation of Eq. (15) is

$$e^{\varepsilon(t)} = \frac{\tau(t)}{1-\tau(t)} \tag{16}$$

Furthermore, there is

$$\tau(t) = \frac{e^{\varepsilon(t)}}{1+e^{\varepsilon(t)}} \tag{17}$$

It can be available form Eq. (17) that

$$0 < \frac{e^{-\varepsilon_M}}{1+e^{-\varepsilon_M}} \le \tau(t) \le \frac{e^{\varepsilon_M}}{1+e^{\varepsilon_M}} < 1 \tag{18}$$

Because of Eq. (18), there is

$$0 < \frac{e(t) - \vartheta_l(t)}{\vartheta_r(t) - \vartheta_l(t)} < 1 \tag{19}$$

that is $\vartheta_l(t) < e(t) < \vartheta_r(t)$.Therefore, the theorem is proved completed.

It should be pointed out that the transient performance is an inherent performance of the control system, which is related to the composition of the control system and the selection of design parameters. Therefore, prescribed performance control does not improve the inherent transient performance of the control system, but only provides a constraint tool to select the desired transient performance through the "squeeze" method.

III. CONTROLLER DESIGN

According to the timescale principle in [44], the velocity is slower dynamics compared with altitude angles. Thus, the HFV motion model can be decomposed into velocity subsystem and altitude subsystem for the simplicity of control design. The HFV longitudinal model (1)∼(7) can be expressed as the nonaffine model

$$\begin{cases} \dot{V} = f_V(V, \Phi) \\ \dot{h} = f_1(\gamma) \\ \dot{\gamma} = f_2(h, \gamma, \theta) \\ \dot{\theta} = Q \\ \dot{Q} = f_3(h, \gamma, \theta, Q, \delta_e) \end{cases} \tag{20}$$

where $f_V(V, \Phi)$ and $f_i(\cdot), i = 1, 2, 3$ are unknown smooth functions.

A. ALTITUDE CONTROLLER DESIGN

Define the altitude performance function as Eq. (12) and the reference input of path angle as

$$\gamma_d = \arcsin[\frac{-k_h\varepsilon_h(t)+\dot{h}_{ref}}{V} - \frac{\vartheta_{lh}(t)\dot{\vartheta}_{rh}(t)-\dot{\vartheta}_{lh}(t)\vartheta_{rh}(t)-e_h\left(\dot{\vartheta}_{rh}(t)-\dot{\vartheta}_{lh}(t)\right)}{V(\vartheta_{rh}(t)-\vartheta_{lh}(t))}] \tag{21}$$

where $k_h > 0$ is a design parameter, $e_h = h - h_{ref}$. If $\gamma \to \gamma_d$, there is the corresponding dynamics for $\varepsilon_h(t)$ as

$$k_h\dot{\varepsilon}_h(t) + \varepsilon_h(t) = 0 \tag{22}$$

Thus, $\varepsilon_h(t)$ is bounded and then the altitude subsystem's control objective becomes $\gamma \to \gamma_d$.

Let $z_1 = x_1 = \gamma, z_2 = \dot{z}_1, x_2 = \theta, x_3 = Q$. From Eq. (20), there is

$$\begin{aligned}\dot{z}_2 &= \dot{f}_2 \\ &= \frac{\partial f_2(x_1,x_2)}{\partial x_1}\dot{x}_2 + \frac{\partial f_2(x_1,x_2)}{\partial x_2}\dot{x}_2 \\ &= \frac{\partial f_2(x_1,x_2)}{\partial x_1}f_2 + \frac{\partial f_2(x_1,x_2)}{\partial x_2}x_3 f_1'(\boldsymbol{x})\end{aligned} \tag{23}$$

where $\boldsymbol{x} = [x_1, x_2, x_3]$.

Assumption 2 (see [38]): For any $(\boldsymbol{x}, \delta_e) \in \Omega_x \times \mathbf{R}$, there is

$$\begin{cases}\dfrac{\partial f_2(x_1,x_2)}{\partial x_2} > 0 \\ \dfrac{\partial f_3(\boldsymbol{x},\delta_e)}{\partial \delta_e} > 0\end{cases} \tag{24}$$

where Ω_x is a controllable set. And $z_3 = \dot{z}_2$, from Eq. (20), there is

$$\begin{aligned}\dot{z}_3 &= \frac{\partial f_1'(\boldsymbol{x})}{\partial x_1}\dot{x}_1 + \frac{\partial f_1'(\boldsymbol{x})}{\partial x_2}\dot{x}_2 + \frac{\partial f_1'(\boldsymbol{x})}{\partial x_3}\dot{x}_3 \\ &= \frac{\partial f_1'(\boldsymbol{x})}{\partial x_1}f_2(x_1,x_2) + \frac{\partial f_1'(\boldsymbol{x})}{\partial x_2}x_3 \\ &\quad + \frac{\partial f_1'(\boldsymbol{x})}{\partial x_3}f_3(\boldsymbol{x},\delta_e) \\ &\triangleq f_2'(\boldsymbol{x},\delta_e)\end{aligned} \tag{25}$$

Thus, after the above transformation, the altitude subsystem is transformed into the following nonaffine pure feedback model.

$$\begin{cases}\dot{z}_1 = z_2 \\ \dot{z}_2 = z_3 \\ \dot{z}_3 = f_2'(\boldsymbol{x},\delta_e)\end{cases} \tag{26}$$

Considering actuator failures and bounded disturbance varying with time, the system (26) becomes

$$\begin{cases}\dot{z}_1 = z_2 \\ \dot{z}_2 = z_3 \\ \dot{z}_3 = f_0'(\boldsymbol{x}) + f_0(\boldsymbol{x},\delta_e) + d_0(t)\end{cases} \tag{27}$$

TABLE 1. Value range of HFV flight envelope.

State	Lower bound	Upper bound
V	2 286 m/s	3 353 m/s
h	25 908 m	41 148 m
γ	-5°	5°
θ	-10°	10°
Q	-10°/s	10°/s
$\bar{q}$	23 940 Pa	95 760 Pa
Φ	0.05	1.5
δ_e	-20°	20°

where $f_0'(\boldsymbol{x})$ is unknown smooth nonlinear function, $f_0(\boldsymbol{x},\delta_e)$ denotes the actuator failures function and $d_0(t)$ denotes bounded disturbance with time. The actuator partial failures can be expressed as $u^f = Au$ with $A \in \mathbf{R}^{n\times n}$ [28], [45]. Also, actuator failures can be expressed as $u^f = (1-\lambda_i)\chi_i$ with $0 < \lambda_i < 1$ and χ_i denotes stuck position [46], [47]. In terms of actual flight, actuator failures cannot be described as a linearized form, but as $u^f = f(\boldsymbol{x},u), t \geq t_f$. t_f is the time when an unknown failure occurs. This failure model is a nonaffine form, which can also be called non-modeling failure.

Assumption 3 (see [48]): There is an unknown positive constant d_0^*, such that $|d_0(t)| \leq d_0^*$.

Assumption 4 (see [49]): $f_0(\boldsymbol{x},\delta_e)$ is differentiable for δ_e. There are unknown positive constants g_0, g_1 and g_2, such that $g(\boldsymbol{x},\delta_e^*) = [\partial f_0(\boldsymbol{x},\delta_e)/\partial\delta_e]\big|_{\delta_e^*=\delta_e}$, $\delta_e^* \in (0,\delta_e)$ satisfies the following inequation

$$\begin{cases}g_0 \leq g(\boldsymbol{x},\delta_e^*) \leq g_1 \\ |g(\boldsymbol{x},\delta_e^*)| \leq g_2\end{cases} \tag{28}$$

According to [38] and the rigid body value range of HFV flight envelope in TAB. 1, Assumptions 2 and 4 are valid.

Based on unconstrained transform error signal, an adaptive fault-tolerant control method is designed by combining RBF neural network with backstepping control. The design process is as follows.

Step 1: Define the flight path angle tracking error $e_\gamma = z_1 - \gamma_d$, and the time derivative of the corresponding transform error is as follows

$$\dot{\varepsilon}_1(t) = r_1(t)[z_2 - \dot{\gamma}_d + \frac{\vartheta_{l1}(t)\dot{\vartheta}_{r1}(t)-\dot{\vartheta}_{l1}(t)\vartheta_{r1}(t)}{\vartheta_{r1}(t)-\vartheta_{l1}(t)} - \frac{e_\gamma\left(\dot{\vartheta}_{r1}(t)-\dot{\vartheta}_{l1}(t)\right)}{\vartheta_{r1}(t)-\vartheta_{l1}(t)}] \tag{29}$$

where $\vartheta_{l1}(t)$ and $\vartheta_{r1}(t)$ are the corresponding performance functions to $\varepsilon_1(t)$, $r_1(t) = \frac{1}{(1-\tau_1(t))(\vartheta_{r1}(t)-\vartheta_{l1}(t))\tau_1(t)} > 0$, $\tau_1(t) = \left[e_\gamma - \vartheta_{l1}(t)\right]/[\vartheta_{r1}(t) - \vartheta_{l1}(t)]$.

Choose the following Lyapunov functional

$$L_1 = \frac{[\varepsilon_1(t)]^2}{2} \tag{30}$$

Differentiation of Eq. (30) is

$$\dot{L}_1 = \varepsilon_1(t)\,\dot{\varepsilon}_1(t) \tag{31}$$

Define the pitch angle tracking error $e_\theta = z_2 - \theta_d$. In combination (29), Eq. (31) can be changed to

$$\begin{aligned}\dot{L}_1 &= \varepsilon_1(t)\,r_1(t)\,[z_2 - \dot{\gamma}_d \\ &\quad + \frac{\vartheta_{l1}(t)\,\dot{\vartheta}_{r1}(t) - \dot{\vartheta}_{l1}(t)\,\vartheta_{r1}(t)}{\vartheta_{r1}(t) - \vartheta_{l1}(t)} \\ &\quad - \frac{e_\gamma\left(\dot{\vartheta}_{r1}(t) - \dot{\vartheta}_{l1}(t)\right)}{\vartheta_{r1}(t) - \vartheta_{l1}(t)}] \\ &= \varepsilon_1(t)\,r_1(t)\,[e_\theta + \theta_d - \dot{\gamma}_d \\ &\quad + \frac{\vartheta_{l1}(t)\,\dot{\vartheta}_{r1}(t) - \dot{\vartheta}_{l1}(t)\,\vartheta_{r1}(t)}{\vartheta_{r1}(t) - \vartheta_{l1}(t)} \\ &\quad - \frac{e_\gamma\left(\dot{\vartheta}_{r1}(t) - \dot{\vartheta}_{l1}(t)\right)}{\vartheta_{r1}(t) - \vartheta_{l1}(t)}] \\ &\le \varepsilon_1(t)\,r_1(t)\,[e_\theta + \theta_d - \dot{\gamma}_d \\ &\quad + \frac{\vartheta_{l1}(t)\,\dot{\vartheta}_{r1}(t) - \dot{\vartheta}_{l1}(t)\,\vartheta_{r1}(t)}{\vartheta_{r1}(t) - \vartheta_{l1}(t)} \\ &\quad - \frac{e_\gamma\left(\dot{\vartheta}_{r1}(t) - \dot{\vartheta}_{l1}(t)\right)}{\vartheta_{r1}(t) - \vartheta_{l1}(t)}] + \frac{[r_1(t)\,\varepsilon_1(t)]^2}{2}\end{aligned} \tag{32}$$

where θ_d is the first virtual control law.

Choose the following virtual control law

$$\begin{aligned}\theta_d &= -\left(\frac{k_1}{r_1(t)} + \frac{r_1(t)}{2} - \frac{1}{2r_1}\right)\varepsilon_1(t) \\ &\quad + \dot{\gamma}_d - \frac{\vartheta_{l1}(t)\,\dot{\vartheta}_{r1}(t) - \dot{\vartheta}_{l1}(t)\,\vartheta_{r1}(t)}{\vartheta_{r1}(t) - \vartheta_{l1}(t)} \\ &\quad + \frac{e_\gamma\left(\dot{\vartheta}_{r1}(t) - \dot{\vartheta}_{l1}(t)\right)}{\vartheta_{r1}(t) - \vartheta_{l1}(t)}\end{aligned} \tag{33}$$

where $k_1 > 1/2$ is a design parameter.

Substituting Eq. (33) into (32), there is

$$\dot{L}_1 \le -\left(k_1 - \frac{1}{2}\right)[\varepsilon_1(t)]^2 + r_1(t)\,\varepsilon_1(t)\,e_\theta \tag{34}$$

Apparently, if e_θ is small enough, there is $\dot{L}_1 \le -(2k_1+1)\,L_1$. Thus, exponential asymptotic convergence of L_1 can be guaranteed.

Step 2: Choose the following Lyapunov functional

$$L_2 = \frac{e_\theta^2}{2} \tag{35}$$

Differentiation of Eq. (35) is

$$\dot{L}_2 = e_\theta \dot{e}_\theta = e_\theta\left(z_3 - \dot{\theta}_d\right) \tag{36}$$

Define the pitch rate tracking error $e_Q = z_3 - Q_d$. Then Eq. (36) becomes

$$\dot{L}_2 = e_\theta \dot{e}_\theta = e_\theta\left(e_Q + Q_d - \dot{\theta}_d\right) \tag{37}$$

where Q_d is the second virtual control law.

Choose the following virtual control law

$$Q_d = -k_2 e_\theta - r_1(t)\,\varepsilon_1(t) + \dot{\theta}_d \tag{38}$$

where $k_2 > 1/2$ is a design parameter.

Substituting Eq. (38) into (37), there is

$$\dot{L}_2 \le -\left(k_2 - \frac{1}{2}\right)e_\theta^2 - r_1(t)\,\varepsilon_1(t)\,e_\theta + e_\theta e_Q \tag{39}$$

Step 3: Considering the pitch rate tracking error $e_Q = z_3 - Q_d$, according to Eq. (27), there is

$$\dot{e}_Q = f_0'(\boldsymbol{x}) + f_0(\boldsymbol{x}, \delta_e) + d_0(t) - \dot{Q}_d \tag{40}$$

According to Mean Value Theorem, Eq. (40) can be expressed as

$$\dot{e}_Q = f_0'(\boldsymbol{x}) + f_0(\boldsymbol{x}, 0) + g\left(\boldsymbol{x}, \delta_e^*\right)\delta_e + d_0(t) - \dot{Q}_d \tag{41}$$

Thus, from Assumption 4, there are $g_0 \le g\left(\boldsymbol{x}, \delta_e^*\right) \le g_1$ and $g\left(\boldsymbol{x}, \delta_e^*\right) > 0$.

Choose the following Lyapunov functional

$$L_3 = \frac{e_Q^2}{2g\left(\boldsymbol{x}, \delta_e^*\right)} \tag{42}$$

Differentiation of Eq. (42) is

$$\begin{aligned}\dot{L}_3 &= \frac{1}{g\left(\boldsymbol{x}, \delta_e^*\right)} e_Q \dot{e}_Q - \frac{\dot{g}\left(\boldsymbol{x}, \delta_e^*\right)}{2g^2\left(\boldsymbol{x}, \delta_e^*\right)} e_Q^2 \\ &= \frac{1}{g\left(\boldsymbol{x}, \delta_e^*\right)} e_Q [f_0'(\boldsymbol{x}) + f_0(\boldsymbol{x}, 0) + g\left(\boldsymbol{x}, \delta_e^*\right)\delta_e \\ &\quad + d_0(t) - \dot{Q}_d] - \frac{\dot{g}\left(\boldsymbol{x}, \delta_e^*\right)}{2g^2\left(\boldsymbol{x}, \delta_e^*\right)} e_Q^2 \\ &= e_Q [\frac{1}{g\left(\boldsymbol{x}, \delta_e^*\right)}\left(f_0'(\boldsymbol{x}) + f_0(\boldsymbol{x}, 0) - \dot{Q}_d\right) \\ &\quad + \delta_e + \frac{d_0(t)}{g\left(\boldsymbol{x}, \delta_e^*\right)}] - \frac{\dot{g}\left(\boldsymbol{x}, \delta_e^*\right)}{2g^2\left(\boldsymbol{x}, \delta_e^*\right)} e_Q^2\end{aligned} \tag{43}$$

According to Lemma 1, applying RBF neural network to approximate $\frac{1}{g(\boldsymbol{x}, \delta_e^*)}\left(f_0'(\boldsymbol{x}) + f_0(\boldsymbol{x}, 0) - \dot{Q}_d\right)$

$$F_h(\boldsymbol{Z}_1) = \frac{1}{g\left(\boldsymbol{x}, \delta_e^*\right)}\left(f_0'(\boldsymbol{x}) + f_0(\boldsymbol{x}, 0) - \dot{Q}_d\right) \tag{44}$$

where $\boldsymbol{Z}_1 = \left[\boldsymbol{x}^T, \dot{Q}_d\right]^T$. Then Eq. (43) becomes

$$\begin{aligned}\dot{L}_3 &= e_Q\left[\boldsymbol{W}_1^{*T} S_1(\boldsymbol{Z}_1) + \delta_1 + \delta_e + \frac{d_0(t)}{g\left(\boldsymbol{x}, \delta_e^*\right)}\right] \\ &\quad - \frac{\dot{g}\left(\boldsymbol{x}, \delta_e^*\right)}{2g^2\left(\boldsymbol{x}, \delta_e^*\right)} e_Q^2 \\ &= e_Q\left[\tilde{\boldsymbol{W}}_1^T S_1(\boldsymbol{Z}_1) + \hat{\boldsymbol{W}}_1^T S_1(\boldsymbol{Z}_1) + \delta_1 + \delta_e + \frac{d_0(t)}{g\left(\boldsymbol{x}, \delta_e^*\right)}\right] \\ &\quad - \frac{\dot{g}\left(\boldsymbol{x}, \delta_e^*\right)}{2g^2\left(\boldsymbol{x}, \delta_e^*\right)} e_Q^2\end{aligned} \tag{45}$$

where $\tilde{\boldsymbol{W}}_1 = \boldsymbol{W}_1^* - \hat{\boldsymbol{W}}_1$. Let $g_2' = g_2/2g_0^2$, and Eq. (45) becomes

$$\begin{aligned}\dot{L}_3 &\le e_Q\left[\tilde{\boldsymbol{W}}_1^T S_1(\boldsymbol{Z}_1) + \hat{\boldsymbol{W}}_1^T S_1(\boldsymbol{Z}_1) + \delta_1 + \delta_e + g_2' e_Q\right] \\ &\quad - \frac{\dot{g}\left(\boldsymbol{x}, \delta_e^*\right)}{2g^2\left(\boldsymbol{x}, \delta_e^*\right)} e_Q^2\end{aligned} \tag{46}$$

Choose the following actual control law and adaptive laws

$$\begin{cases} \delta_e = -k_3 e_Q - \hat{\boldsymbol{W}}_1^T S_1(\boldsymbol{Z}_1) - e_\theta - \hat{g}_2' e_Q \\ \dot{\hat{\boldsymbol{W}}}_1 = c_0 e_Q S_1(\boldsymbol{Z}_1) + c_1 \hat{\boldsymbol{W}}_1 \\ \dot{\hat{g}}_2' = c_2 e_Q^2 + c_3 \hat{g}_2' \end{cases} \tag{47}$$

where $\hat{g}_2'$ is the estimation of g_2'. k_3, c_0, c_1, c_2 and c_3 are positive design parameters.

Substituting Eqs. (44) and (47) into (45), there is

$$\dot{L}_3 \le -k_3 e_Q^2 + e_Q \tilde{\boldsymbol{W}}_1^T S_1(\boldsymbol{Z}_1) + e_Q \delta_1 - e_\theta e_Q + \tilde{g}_2' e_Q^2 + \frac{d_0(t)}{g\left(\boldsymbol{x}, \delta_e^*\right)} e_Q \tag{48}$$

Theorem 2: Considering HFV altitude subsystem with unmodeled actuator failures and bounded disturbances, on the premise of satisfying Assumptions 1 ∼ 4, the fault-tolerant control law and adaptive laws in Eq. (47) are designed by transform error. All signals in the closed-loop system are bounded and the tracking error is limited to the prescribed range.

Proof: According to the derivation process, choose the following Lyapunov functional

$$L_0 = L_1 + L_2 + L_3 + \frac{1}{2c_0} \tilde{\boldsymbol{W}}_1^T \tilde{\boldsymbol{W}}_1 + \frac{1}{2c_2} \tilde{g}_2'^2 \tag{49}$$

Differentiation of Eq. (49) is

$$\dot{L}_0 = \dot{L}_1 + \dot{L}_2 + \dot{L}_3 + \frac{1}{c_0} \tilde{\boldsymbol{W}}^T \dot{\tilde{\boldsymbol{W}}} + \frac{1}{c_2} \tilde{g}_2' \dot{\tilde{g}}_2' \tag{50}$$

According to Eqs. (34), (39) and (46), there is

$$\begin{aligned} \dot{L}_0 \le & -k_1 [\varepsilon_1(t)]^2 - k_2 e_\theta^2 - k_3 e_Q^2 \\ & + \left(\frac{1}{2} - \frac{[r_1(t)]^2}{2} \right) [\varepsilon_1(t)]^2 + e_Q \left(\tilde{\boldsymbol{W}}_1^{\mathrm{T}} S_1(\boldsymbol{Z}_1) + \delta_1 \right) \\ & + \tilde{g}_2' e_Q^2 + \frac{d_0(t)}{g\left(\mathbf{x}, \delta_e^*\right)} e_Q + \frac{1}{c_0} \tilde{\boldsymbol{W}}_1^{\mathrm{T}} \dot{\tilde{\boldsymbol{W}}}_1 + \frac{1}{c_2} \tilde{g}_2' \dot{\tilde{g}}_2' \end{aligned} \tag{51}$$

Using Lemma 1 and Assumption 3∼4, there is

$$\begin{aligned} \dot{L}_0 \le & -\left(k_1 - \frac{1}{2} \right) [\varepsilon_1(t)]^2 - \left(k_2 - \frac{1}{2} \right) e_\theta^2 - (k_3 - 1) e_Q^2 \\ & + e_Q \tilde{\boldsymbol{W}}_1^{\mathrm{T}} S_1(\boldsymbol{Z}_1) + \frac{1}{2} \delta_{1M}^2 \\ & + \tilde{g}_2' e_Q^2 + \frac{d_0^{*2}}{2g_0^2} + \frac{1}{c_0} \tilde{\boldsymbol{W}}_1^{\mathrm{T}} \dot{\tilde{\boldsymbol{W}}}_1 - \frac{1}{c_2} \tilde{g}_2' \dot{\tilde{g}}_2' \end{aligned} \tag{52}$$

Substituting Eq. (47) into (52), there is

$$\begin{aligned} \dot{L}_0 \le & -\left(k_1 - \frac{1}{2} \right) [\varepsilon_1(t)]^2 - \left(k_2 - \frac{1}{2} \right) e_\theta^2 \\ & - (k_3 - 1) e_Q^2 + \frac{1}{2} \delta_{1M}^2 + \frac{d_0^{*2}}{2g_0^2} \\ & - \frac{c_1}{c_0} \tilde{W}_1^{\mathrm{T}} \hat{\tilde{W}}_1 - \frac{c_3}{c_2} \tilde{g}_2' \dot{\tilde{g}}_2' \end{aligned} \tag{53}$$

There are inequalities as follows

$$\begin{cases} -\frac{c_1}{c_0} \tilde{\boldsymbol{W}}_1^{\mathrm{T}} \dot{\tilde{\boldsymbol{W}}}_1 \le -\frac{c_1}{2c_0} \left\| \tilde{\boldsymbol{W}}_1 \right\|^2 + \frac{c_1}{2c_0} \overline{\boldsymbol{W}}_1^2 \\ -\frac{c_3}{c_2} \tilde{g}_2' \hat{g}_2' \le -\frac{c_3}{2c_2} \left\| \tilde{g}_2' \right\|^2 + \frac{c_3}{2c_2} \left\| \hat{g}_2' \right\|^2 \end{cases} \tag{54}$$

where $\overline{\boldsymbol{W}}_1$ is a design parameter.

Substituting Eq. (54) into (53), there is

$$\begin{aligned} \dot{L}_0 \le & -\left(k_1 - \frac{1}{2} \right) [\varepsilon_1(t)]^2 - \left(k_2 - \frac{1}{2} \right) e_\theta^2 \\ & - (k_3 - 1) e_Q^2 + \frac{d_0^{*2}}{2g_0^2} + \frac{1}{2} \delta_{1M}^2 \\ & - \frac{c_1}{2c_0} \left\| \tilde{\boldsymbol{W}}_1 \right\|^2 + \frac{c_1}{2c_0} \overline{\boldsymbol{W}}_1^2 + \frac{c_3}{2c_2} \left\| \hat{g}_2' \right\|^2 - \frac{c_3}{2c_2} \left\| \tilde{g}_2' \right\|^2 \\ \le & -\dot{\varkappa}_1 L_0 + \ell_1 \end{aligned} \tag{55}$$

where $\dot{\varkappa}_1 = \min\left\{ \left(k_1 - \frac{1}{2} \right), \left(k_2 - \frac{1}{2} \right), (k_3 - 1), \frac{c_1}{2c_0}, \frac{c_3}{2c_2} \right\}$, $\ell_1 = \frac{c_1}{2c_0} \overline{\boldsymbol{W}}_1^2 + \frac{c_3}{2c_2} \left\| \hat{g}_2' \right\|^2 + \frac{d_0^{*2}}{2g_0^2} + \frac{1}{2} \delta_{1M}^2$. When $k_3 > 1$,the integral of Eq. (55) is

$$L_0(t) \le \ell_1 / \dot{\varkappa}_1 + [L_0(0) - \ell_1 / \dot{\varkappa}_1] e^{-\dot{\varkappa}_1 t} \tag{56}$$

From Eq. (56), $L_0(t)$ is exponential asymptotic convergence and $\lim_{t \to \infty} L_0(t) = \ell_1 / \dot{\varkappa}_1$. It can be obviously seen that e_Q and $\tilde{\boldsymbol{W}}_1$ are uniformly ultimately bound. Thus, e_θ is bounded. And then the transform error $\varepsilon_1(t)$ is uniformly ultimately bound. From Theorem 1, the tracking error is limited to the prescribed range as Eq. (13). Therefore, the theorem is proved completed.

B. VELOCITY CONTROLLER DESIGN

Considering the actuator failures and bounded disturbance in the actual flight process of HFV, the velocity subsystem in Eq. (20) is changed into the following form:

$$\dot{V} = f_V'(V, \Phi) + f_{V0}(V, \Phi) + d_{V0}(t) \tag{57}$$

where $f_V'(V, \Phi)$ is an unknown smooth nonlinear function, $f_{V0}(V, \Phi)$ denotes the actuator failures function and $d_{V0}(t)$ denotes bounded disturbance with time.

Assumption 5 (see [48]): There is an unknown positive constant d_{V0}^*, such that $|d_{V0}(t)| \le d_{V0}^*$.

Assumption 6 (see [49]): $f_{V0}(V, \Phi)$ is differentiable for Φ. There are unknown positive constants g_{V0}, g_{V1} and g_{V2}, such that $g_V(V, \Phi^*) = [\partial f_{V0}(V, \Phi) / \partial \Phi]|_{\Phi^* = \Phi}$. $\Phi^* \in (0, \Phi)$ satisfies the following inequation

$$\begin{cases} g_{V0} \le g_V(V, \Phi^*) \le g_{V1} \\ |g_V(V, \Phi^*)| \le g_{V2} \end{cases} \tag{58}$$

According to the design method of altitude subsystem controller, the following adaptive fault-tolerant control law is designed for velocity subsystem.

Define the velocity tracking error $e_V = V - V_{ref}$, and the derivative of the corresponding transform error is

as follows

$$\dot{\varepsilon}_2(t) = r_2(t)[f'_V(V,\Phi) + f_{V0}(V,\Phi) + d_{V0}(t) - \dot{V}_{ref} + \frac{\vartheta_{l2}(t)\dot{\vartheta}_{r2}(t) - \dot{\vartheta}_{l2}(t)\vartheta_{r2}(t)}{\vartheta_{r2}(t) - \vartheta_{l2}(t)} - \frac{e_V\left(\dot{\vartheta}_{r2}(t) - \dot{\vartheta}_{l2}(t)\right)}{\vartheta_{r2}(t) - \vartheta_{l2}(t)}] \tag{59}$$

where

$$\begin{cases} \vartheta_{l2}(t) = [\tanh(e_V) - 1/2]\vartheta_2(t) - \tanh(e_V)\vartheta_{2\infty} \\ \vartheta_{r2}(t) = [\tanh(e_V) + 1/2]\vartheta_2(t) - \tanh(e_V)\vartheta_{2\infty} \\ \varepsilon_2(t) = \ln(\tau_2(t)/(1-\tau_2(t))) \\ \tau_2(t) = [e_V - \vartheta_{l2}(t)]/[\vartheta_{r2}(t) - \vartheta_{l2}(t)] \\ \vartheta_2(t) = (\vartheta_{20} - \vartheta_{2\infty})e^{-l_2 t} + \vartheta_{2\infty} \end{cases}$$

with ϑ_{20}, $\vartheta_{2\infty}$ and l_2 are design parameters.

According to the Mean Value Theorem, Eq. (59) can be rewritten as

$$\dot{\varepsilon}_2(t) = r_2(t)[f'_V(V,\Phi) + f_{V0}(V,0) + g_V\left(V,\Phi^*\right)\Phi + d_{V0}(t) - \dot{V}_{ref} + \frac{\vartheta_{l2}(t)\dot{\vartheta}_{r2}(t) - \dot{\vartheta}_{l2}(t)\vartheta_{r2}(t)}{\vartheta_{r2}(t) - \vartheta_{l2}(t)} - \frac{e_V\left(\dot{\vartheta}_{r2}(t) - \dot{\vartheta}_{l2}(t)\right)}{\vartheta_{r2}(t) - \vartheta_{l2}(t)}] \tag{60}$$

Thus, from Assumption 6, we may know $g_{V0} \le g_V(V,\Phi^*) \le g_{V1}$, $g_V(V,\Phi^*) > 0$.

Choose the following Lyapunov functional

$$L_V = \frac{1}{2g_V(V,\Phi^*)}[\varepsilon_2(t)]^2 \tag{61}$$

Differentiation of Eq. (61) is

$$\begin{aligned} L_V &= \frac{1}{g_V(V,\Phi^*)}\varepsilon_2(t)\dot{\varepsilon}_2(t) - \frac{\dot{g}_V(V,\Phi^*)}{2g_V^2(V,\Phi^*)}[\varepsilon_2(t)]^2 \\ &= \frac{1}{g_V(V,\Phi^*)}\varepsilon_2(t)r_2(t)\{f'_V(V,\Phi) + f_{V0}(V,0) \\ &\quad + g_V\left(V,\Phi^*\right)\Phi + d_{V0}(t) - \dot{V}_{ref} \\ &\quad + \frac{\vartheta_{l2}(t)\dot{\vartheta}_{r2}(t) - \dot{\vartheta}_{l2}(t)\vartheta_{r2}(t)}{\vartheta_{r2}(t) - \vartheta_{l2}(t)} \\ &\quad - \frac{e_V\left[\dot{\vartheta}_{r2}(t) - \dot{\vartheta}_{l2}(t)\right]}{\vartheta_{r2}(t) - \vartheta_{l2}(t)}\} - \frac{\dot{g}_V(V,\Phi^*)}{2g_V^2(V,\Phi^*)}[\varepsilon_2(t)]^2 \\ &= \varepsilon_2(t)r_2(t)\{\frac{f'_V(V,\Phi) + f_{V0}(V,0) + d_{V0}(t)}{g_V(V,\Phi^*)} \\ &\quad - \frac{\dot{V}_{ref}}{g_V(V,\Phi^*)} + \frac{\vartheta_{l2}(t)\dot{\vartheta}_{r2}(t) - \dot{\vartheta}_{l2}(t)\vartheta_{r2}(t)}{g_V(V,\Phi^*)[\vartheta_{r2}(t) - \vartheta_{l2}(t)]} \\ &\quad - \frac{e_V\left[\dot{\vartheta}_{r2}(t) - \dot{\vartheta}_{l2}(t)\right]}{g_V(V,\Phi^*)[\vartheta_{r2}(t) - \vartheta_{l2}(t)]}\} \\ &\quad + \varepsilon_2(t)r_2(t)\Phi - \frac{\dot{g}_V(V,\Phi^*)}{2g_V^2(V,\Phi^*)}[\varepsilon_2(t)]^2 \end{aligned} \tag{62}$$

According to Lemma 1, applying RBF neural network to approximate actuator failures.

$$F_V(\mathbf{Z}_2) = \frac{f'_V(V,\Phi) + f_{V0}(V,0) - \dot{V}_{ref}}{g_V(V,\Phi^*)} \tag{63}$$

where $\mathbf{Z}_2 = \left[V, \dot{V}_{ref}\right]^T$. Thus, the Eq. (62) is changed into

$$\begin{aligned} \dot{L}_V &= \varepsilon_2(t)r_2(t)\{\boldsymbol{W}_2^{*T}S_2(\mathbf{Z}_2) + o_2 + \Phi + \frac{d_{V0}(t)}{g_V(V,\Phi^*)} \\ &\quad + \frac{\vartheta_{l2}(t)\dot{\vartheta}_{r2}(t) - \dot{\vartheta}_{l2}(t)\vartheta_{r2}(t)}{g_V(V,\Phi^*)[\vartheta_{r2}(t) - \vartheta_{l2}(t)]} \\ &\quad - \frac{e_V\left[\dot{\vartheta}_{r2}(t) - \dot{\vartheta}_{l2}(t)\right]}{g_V(V,\Phi^*)[\vartheta_{r2}(t) - \vartheta_{l2}(t)]}\} \\ &\quad - \frac{\dot{g}_V(V,\Phi^*)}{2g_V^2(V,\Phi^*)}[\varepsilon_2(t)]^2 \\ &= \varepsilon_2(t)r_2(t)\{\tilde{\boldsymbol{W}}_2^{\mathrm{T}}S_2(\mathbf{Z}_2) + \hat{\boldsymbol{W}}_2^{\mathrm{T}}S_2(\mathbf{Z}_2) + \delta_2 \\ &\quad + \Phi + \frac{d_{V0}(t)}{g_V(V,\Phi^*)} + \frac{\vartheta_{l2}(t)\dot{\vartheta}_{r2}(t) - \dot{\vartheta}_{l2}(t)\vartheta_{r2}(t)}{g_V(V,\Phi^*)[\vartheta_{r2}(t) - \vartheta_{l2}(t)]} \\ &\quad - \frac{e_V\left[\dot{\vartheta}_{r2}(t) - \dot{\vartheta}_{l2}(t)\right]}{g_V(V,\Phi^*)[\vartheta_{r2}(t) - \vartheta_{l2}(t)]}\} \\ &\quad - \frac{\dot{g}_V(V,\Phi^*)}{2g_V^2(V,\Phi^*)}[\varepsilon_2(t)]^2 \end{aligned} \tag{64}$$

where $\tilde{\boldsymbol{W}}_2 = \boldsymbol{W}_2^* - \hat{\boldsymbol{W}}_2$. Let $g'_{V2} = g_{V2}/2g_{V0}^2$, Eq. (64) is changed into

$$\begin{aligned} \dot{L}_V &\le \varepsilon_2(t)r_2(t)\{\tilde{\boldsymbol{W}}_2^{\mathrm{T}}S_2(\mathbf{Z}_2) + \hat{\boldsymbol{W}}_2^{\mathrm{T}}S_2(\mathbf{Z}_2) \\ &\quad + \delta_2 + \Phi + \frac{g'_{V2}\varepsilon_2(t)}{r_2(t)} \\ &\quad + \frac{\vartheta_{l2}(t)\dot{\vartheta}_{r2}(t) - \dot{\vartheta}_{l2}(t)\vartheta_{r2}(t)}{g_V(V,\Phi^*)[\vartheta_{r2}(t) - \vartheta_{l2}(t)]} \\ &\quad - \frac{e_V\left[\dot{\vartheta}_{r2}(t) - \dot{\vartheta}_{l2}(t)\right]}{g_V(V,\Phi^*)[\vartheta_{r2}(t) - \vartheta_{l2}(t)]}\} \\ &\quad + \frac{d_{V0}(t)}{g_V(V,\Phi^*)}\varepsilon_2(t)r_2(t) \end{aligned} \tag{65}$$

Choose the following control law and adaptive laws

$$\begin{cases} \Phi = -\left[\frac{k_{V1}}{r_2(t)} + \frac{r_2(t)}{2} - \frac{1}{2r_2(t)}\right]\varepsilon_2(t) - \hat{\boldsymbol{W}}_2^T S_2(\mathbf{Z}_2) \\ -\frac{\hat{g}'_{V2}\varepsilon_2(t)}{r_2(t)} - \frac{\vartheta_{l2}(t)\dot{\vartheta}_{r2}(t) - \dot{\vartheta}_{l2}(t)\vartheta_{r2}(t)}{g_V(V,\Phi^*)[\vartheta_{r2}(t) - \vartheta_{l2}(t)]} \\ + \frac{e_V\left[\dot{\vartheta}_{r2}(t) - \dot{\vartheta}_{l2}(t)\right]}{g_V(V,\Phi^*)[\vartheta_{r2}(t) - \vartheta_{l2}(t)]} \\ \dot{\hat{\boldsymbol{W}}}_2 = c_{V0}\varepsilon_2(t)S_2(\mathbf{Z}_2) + c_{V1}\hat{\boldsymbol{W}}_2 \\ \dot{\hat{g}}'_{V2} = c_{V2}[\varepsilon_2(t)]^2 + c_{V3}\hat{g}'_{V2} \end{cases} \tag{66}$$

where $\hat{g}'_{V2}$ is the estimation of g'_{V2}. $k_{V1} > \frac{1}{2}$, $c_{V0} > 0$, $c_{V1} > 0$, $c_{V2} > 0$ and $c_{V3} > 0$ are design parameters.

Substituting Eqs. (63) and (66) into (65), there is

$$\dot{L}_V \le -\left(k_{V1} + \frac{[r_2(t)]^2}{2} - \frac{1}{2} - g'_{V2}\right)[\varepsilon_2(t)]^2 + \left(\tilde{\boldsymbol{W}}_2^{\mathrm{T}}S_2(\mathbf{Z}_2) + o_2 + \frac{d_{V0}(t)}{g_V(V,\Phi^*)}\right)\varepsilon_2(t)r_2(t) \tag{67}$$

Theorem 3: Considering HFV velocity subsystem with actuator failures and bounded disturbance, on the premise

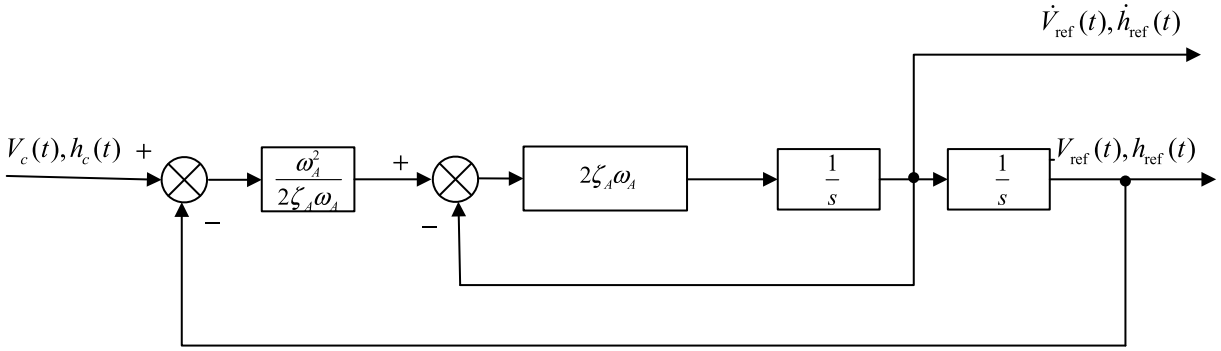

FIGURE 3. Second-order reference model.

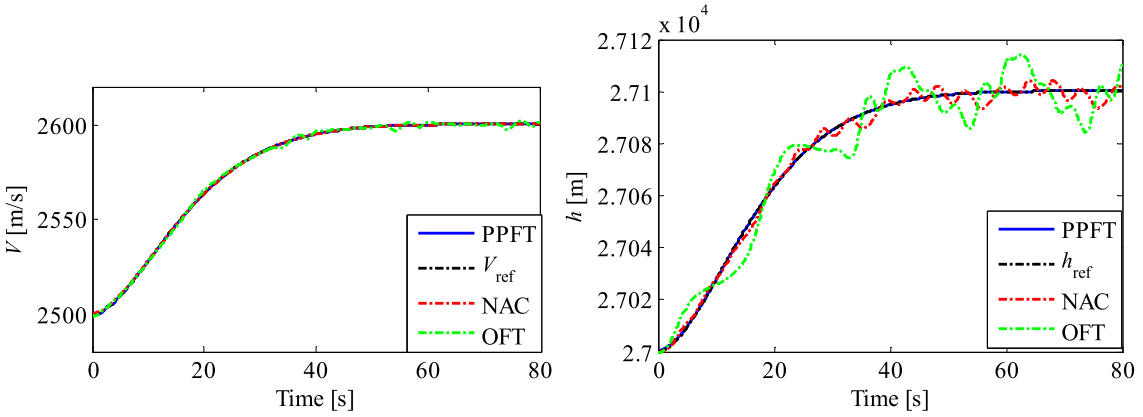

FIGURE 4. Velocity and altitude tracking performance.

TABLE 2. HFV state initial values.

State	Value
V	2500.762m/s
h	27000.159 m
γ	0 deg
θ	1.5295 deg
$\mathcal{Q}$	0 deg/s
η_1	0.2857
η_2	0.2350

of satisfying Assumptions 5 $\sim$ 6, the fault-tolerant control law and adaptive laws in Eq. (66) are designed for the HFV velocity subsystem. The transform error $\varepsilon_2(t)$ in the closed-loop system is bounded, and the velocity tracking error is limited in the prescribed range, so as to realize the prescribed transient performance and steady-state accuracy.

Proof: Consider the following Lyapunov functional

$$L_{V0} = \frac{1}{2g_V(V,\Phi^*)}[\varepsilon_2(t)]^2 + \frac{1}{2c_{V0}}\tilde{\boldsymbol{W}}_2^T\hat{\boldsymbol{W}}_2 + \frac{1}{2c_{V2}}\tilde{g}'_{V2} \tag{68}$$

Differentiation of Eq. (68) is

$$\dot{L}_{V0} = \frac{1}{g_V(V,\Phi^*)}\varepsilon_2(t)\dot{\varepsilon}_2(t) - \frac{\dot{g}_V(V,\Phi^*)}{2g_V^2(V,\Phi^*)}[\varepsilon_2(t)]^2 + \frac{1}{c_{V0}}\tilde{W}_2^T\dot{\tilde{W}}_2 + \frac{1}{c_{V2}}\tilde{g}'_{V2}\dot{\hat{g}}_{V2} \tag{69}$$

According to Eqs. (60) and (67), there is

$$\begin{aligned}\dot{L}_{V0} \le & -k_{V1}[\varepsilon_2(t)]^2 + \left(\frac{1}{2} - \frac{[r_2(t)]^2}{2}\right)[\varepsilon_2(t)]^2 \\ & + \left(\tilde{\boldsymbol{W}}_2^{\mathrm{T}}h_2(\boldsymbol{\ell}_2) + \delta_2\right)\varepsilon_2(t)r_2(t) \\ & + \tilde{g}'_{V2}[\varepsilon_2(t)]^2 + \frac{d_{V0}(t)}{g_V(V,\Phi^*)}\varepsilon_2(t)r_2(t) \\ & + \frac{1}{c_{V0}}\tilde{\boldsymbol{W}}_2^{\mathbf{T}}\dot{\tilde{\boldsymbol{W}}}_2 + \frac{1}{c_{V2}}\tilde{g}'_{V2}\dot{\hat{g}}_{V2}\end{aligned} \tag{70}$$

Using Lemma 1 and Assumptions 5$\sim$6, there is

$$\begin{aligned}\dot{L}_{V0} \le & -\left(k_{V1} - \frac{1}{2}\right)[\varepsilon_2(t)]^2 \\ & + \tilde{\boldsymbol{W}}_2^{\mathrm{T}}h_2(\boldsymbol{\ell}_2)\varepsilon_2(t)r_2(t) + \frac{1}{2}\delta_{2M}^2 \\ & + \tilde{g}'_{V2}[\varepsilon_2(t)]^2 + \frac{d_{V0}^{*2}}{2g_{V0}^2} \\ & + \frac{1}{c_{V0}}\tilde{\boldsymbol{W}}_2^{\mathbf{T}}\dot{\tilde{\boldsymbol{W}}}_2 - \frac{1}{c_{V2}}\tilde{g}'_{V2}\dot{\hat{g}}_{V2}\end{aligned} \tag{71}$$

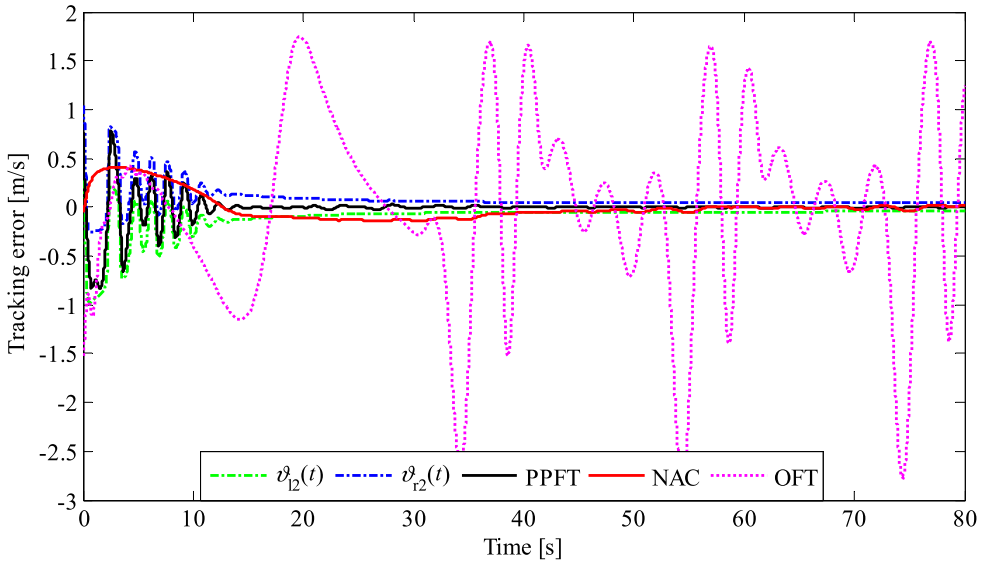

FIGURE 5. Velocity tracking error.

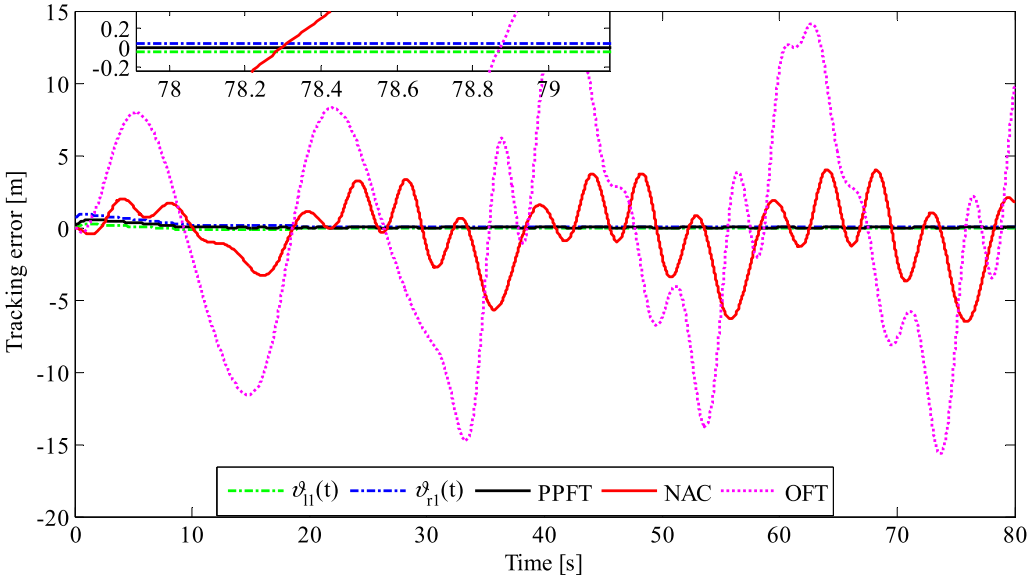

FIGURE 6. Altitude tracking error.

Substituting Eq. (66) into (71), there is

$$\dot{L}_{V0} \leq -\left(k_{V1}-\frac{1}{2}\right)[\varepsilon_2(t)]^2+\frac{1}{2}\delta_{2M}^2 +\frac{d_{V0}^{*2}}{2g_{V0}^2}-\frac{c_{V1}}{c_{V0}}\tilde{\boldsymbol{W}}_2^T\dot{\hat{\boldsymbol{W}}}_2-\frac{c_{V3}}{c_{V2}}\tilde{g}'_{V2}\dot{\hat{g}}_{V2} \quad (72)$$

There are inequalities as follows

$$\begin{cases} -\dfrac{c_{V1}}{c_{V0}}\tilde{\boldsymbol{W}}_2^T\dot{\hat{\boldsymbol{W}}}_2 \leq -\dfrac{c_{V1}}{2c_{V0}}\left\|\tilde{\boldsymbol{W}}_2\right\|^2+\dfrac{c_{V1}}{2c_{V0}}\overline{\boldsymbol{W}}_2^2 \\ -\dfrac{c_{V3}}{c_{V2}}\tilde{g}'_{V2}\dot{\hat{g}}'_{V2} \leq -\dfrac{c_{V3}}{2c_{V2}}\left\|\tilde{g}'_{V2}\right\|^2+\dfrac{c_{V3}}{2c_{V2}}\left\|\hat{g}'_{V2}\right\|^2 \end{cases} \quad (73)$$

where $\overline{\boldsymbol{W}}_2$ is a design parameter.

Substituting Eq. (62) into (72), there is

$$\begin{aligned}\dot{L}_{V0} &\leq -\left(k_{V1}-\frac{1}{2}\right)[\varepsilon_2(t)]^2+\frac{d_{V0}^{*2}}{2g_{V0}^2}+\frac{1}{2}\delta_{2M}^2 \\ &\quad -\frac{c_{V1}}{2c_{V0}}\left\|\tilde{\boldsymbol{W}}_2\right\|^2+\frac{c_{V1}}{2c_{V0}}\overline{\boldsymbol{W}}_2^2 \\ &\quad +\frac{c_{V3}}{2c_{V2}}\left\|\hat{g}'_{V2}\right\|^2-\frac{c_{V3}}{2c_{V2}}\left\|\tilde{g}'_{V2}\right\|^2 \\ &\leq -\bar{\lambda}_2 L_{V0}+\ell_2 \end{aligned} \quad (74)$$

where $\bar{\lambda}_2=\min\left\{\left(k_{V1}-\frac{1}{2}\right),\frac{c_{V1}}{2c_{V0}},\frac{c_{V3}}{2c_{V2}}\right\}$, $\ell_2=\frac{c_{V1}}{2c_{V0}}\overline{\boldsymbol{W}}_2^2+\frac{c_{V3}}{2c_{V2}}\left\|\hat{g}'_{V2}\right\|^2+\frac{d_{V0}^{*2}}{2g_{V0}^2}+\frac{1}{2}\delta_{2M}^2$. The integral of Eq. (74) is

$$L_{V0}(t) \leq \ell_2/\bar{\lambda}_2+[L_{V0}(0)-\ell_2/\bar{\lambda}_2]\,e^{-\bar{\lambda}_2 t} \quad (75)$$

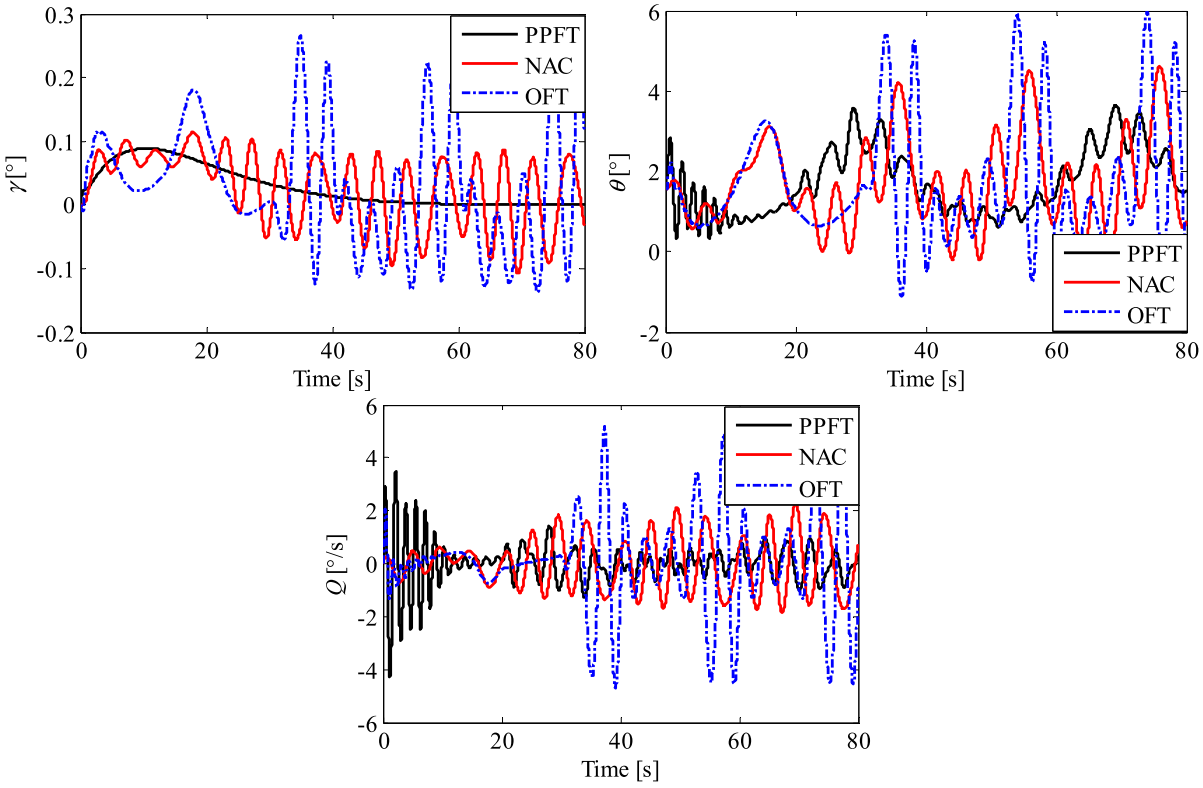

FIGURE 7. Altitude angles.

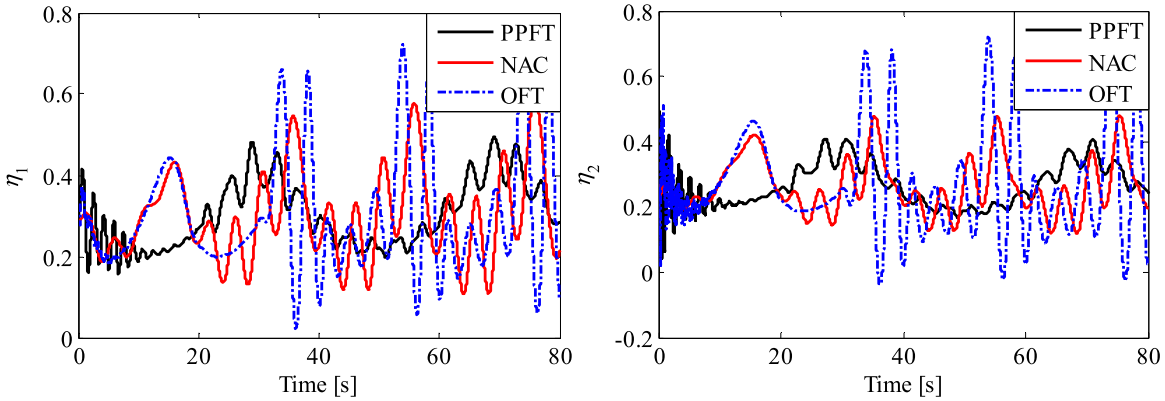

FIGURE 8. Flexible states.

From Eq. (75), $L_{V0}(t)$ is exponential asymptotic convergence and $\lim_{t\to\infty} L_{V0}(t) = \ell_2/\bar{\lambda}_2$. It can be obviously seen that $\tilde{\boldsymbol{W}}_2$ is uniformly ultimately bound. And then the transform error $\varepsilon_2(t)$ is uniformly ultimately bound. From Theorem 1, the tracking error is limited to prescribed range as Eq. (13). Therefore, the theorem is proved completed.

IV. SIMULATION RESULTS

The longitudinal motion model of HFV (1)∼(7) is used to become the controlled object, and the tracking simulation experiment of velocity and altitude reference inputs is carried out by MATLAB. The simulation algorithm is solved by the fourth-order Runge-Kutta method, and the simulation step is 0.01s. The control laws and adaptive laws (33), (38), (47), (66) are used in the simulation experiment. The state initial values of HFV are shown in the Tab. 2. Meanwhile, all the model parameters and aerodynamics coefficients used in this paper can refer to [37] and [38].

In the simulation test, both the velocity and altitude reference models are smoothed via the following filters respectively and same to [50].

$$\frac{V_{ref}(s)}{V_c(s)} = \frac{h_{ref}(s)}{h_c(s)} = \frac{0.1^2}{s^2 + 2 \times 0.9 \times 0.1 \times s + 0.1^2} \tag{76}$$

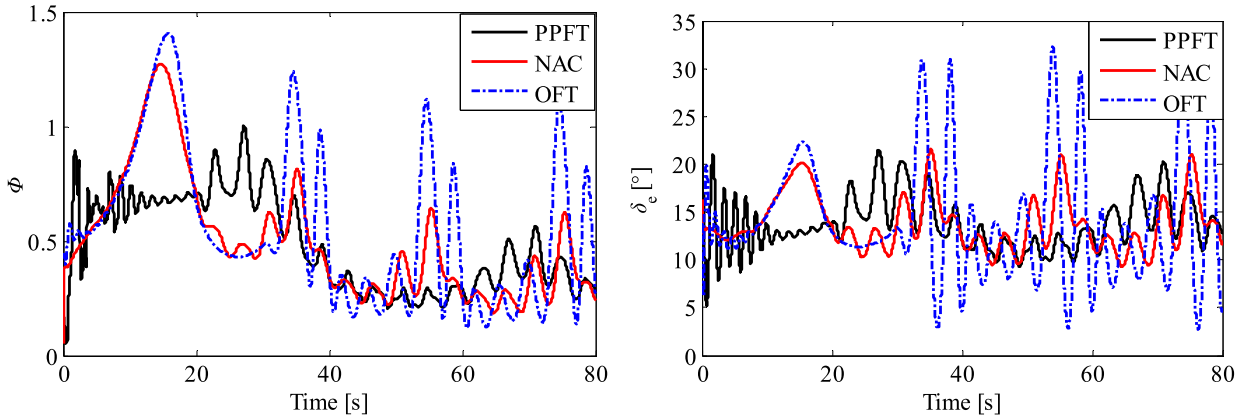

FIGURE 9. Control inputs.

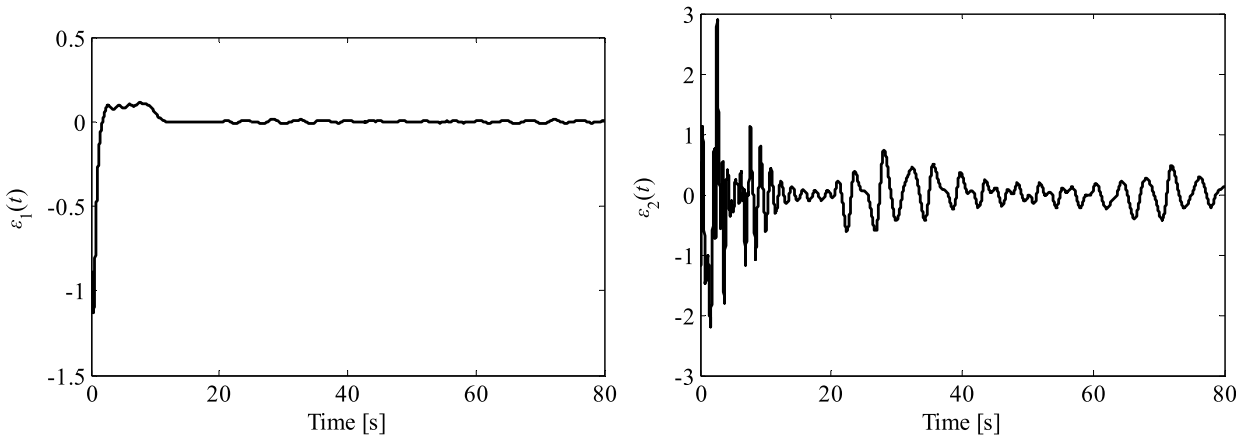

FIGURE 10. Transform error.

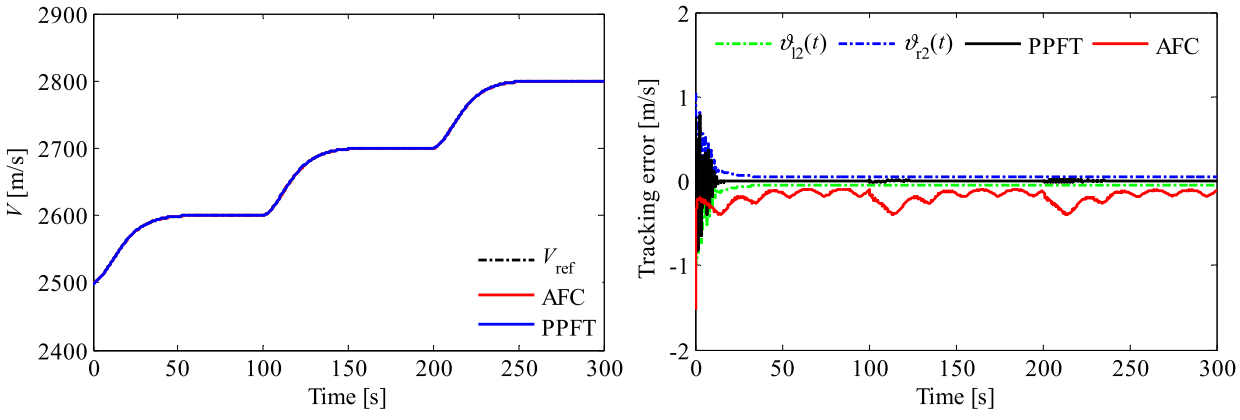

FIGURE 11. Velocity tracking performance.

The second-order reference model given by the (76) is shown in the Fig. 3. In the simulation experiment, the velocity step amplitude V_c is 100m/s and the altitude step amplitude h_c is 100m.

In order to test the robustness of the controller, assuming that the aerodynamic coefficients of the HFV model have perturbations $C = C_0[1 + 0.4\sin(0.05\pi t)]$, where C_0 is nominal value of HFV aerodynamic coefficient. By this

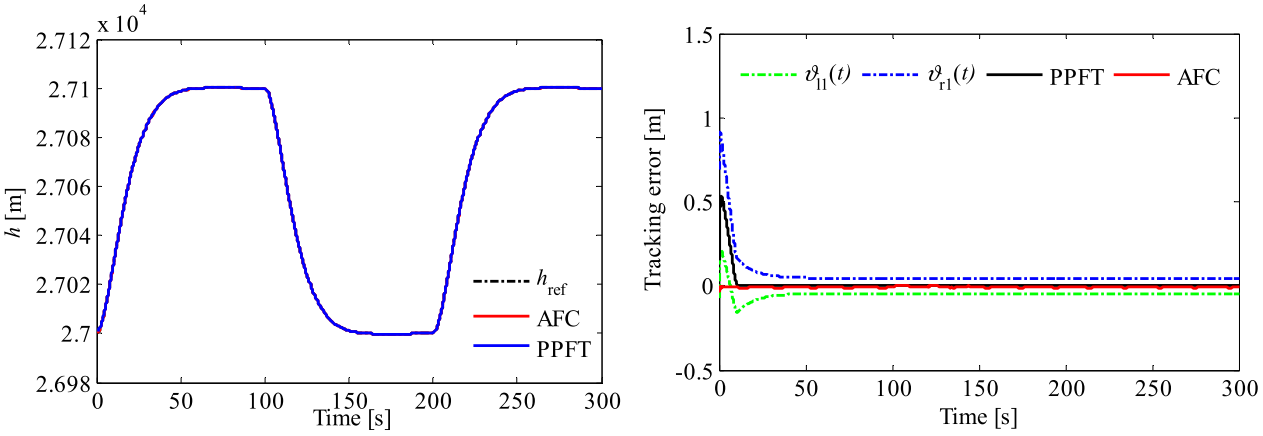

FIGURE 12. Altitude tracking performance.

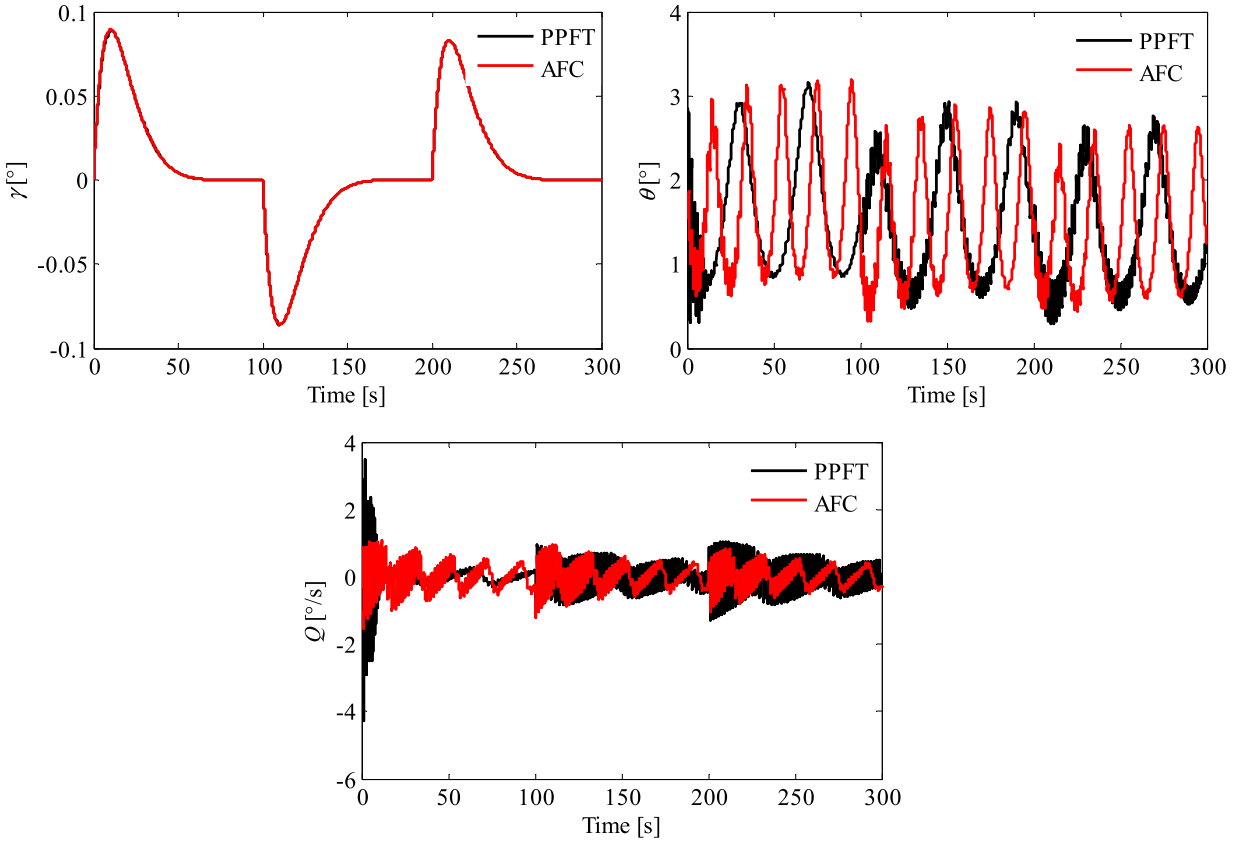

FIGURE 13. Altitude angles.

definition, parameter uncertainty up to 40% of the nominal value is taken into consideration. The performance functions of control system are chosen as:

$$\begin{cases} \vartheta_{l1}(t) = (\tanh e_h - 1/2)\,\vartheta_1(t) - 0.1\tanh(e_h) \\ \vartheta_{r1}(t) = (\tanh e_h + 1/2)\,\vartheta_1(t) - 0.1\tanh(e_h) \\ \vartheta_{l2}(t) = (\tanh e_V - 1/2)\,\vartheta_2(t) - 0.3\tanh(e_V) \\ \vartheta_{r2}(t) = (\tanh e_V + 1/2)\,\vartheta_2(t) - 0.3\tanh(e_V) \\ \vartheta_1(t) = (0.7 - 0.1)\,e^{-0.1t} + 0.1 \\ \vartheta_2(t) = (2.5 - 0.3)\,e^{-0.1t} + 0.3 \end{cases} \tag{77}$$

The controller parameters are chosen as $k_{V1} = 0.8$, $k_1 = 10$, $k_2 = 20$, $k_3 = 20$, $c_0 = 0.1$, $c_1 = 0.1$, $c_2 = 0.05$, $c_3 = 0.05$, $c_{V0} = 0.5$, $c_{V1} = 0.5$, $c_{V2} = 0.1$, $c_{V3} = 0.1$. The nodes number in the neural network of altitude subsystem is chosen as $p = 20$, center point coordinate vectors are averagely distributed in $[-1°, 1°] \times [0°, 5°] \times [-5°/s, 5°/s] \times [0°/s^2, 0.35°/s^2]$, the element of the width vector $\boldsymbol{b}$ is 3.5. The nodes number in the neural network of velocity subsystem is chosen as $p = 20$, center point coordinate vectors are averagely distributed in [2500m/s, 3100m/s]×[−0.1, 1]. The failure

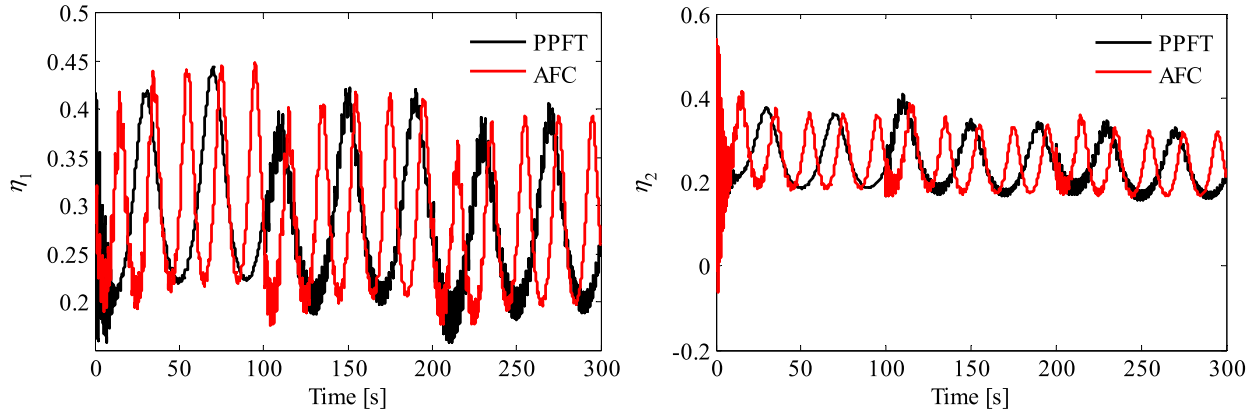

FIGURE 14. Flexible states.

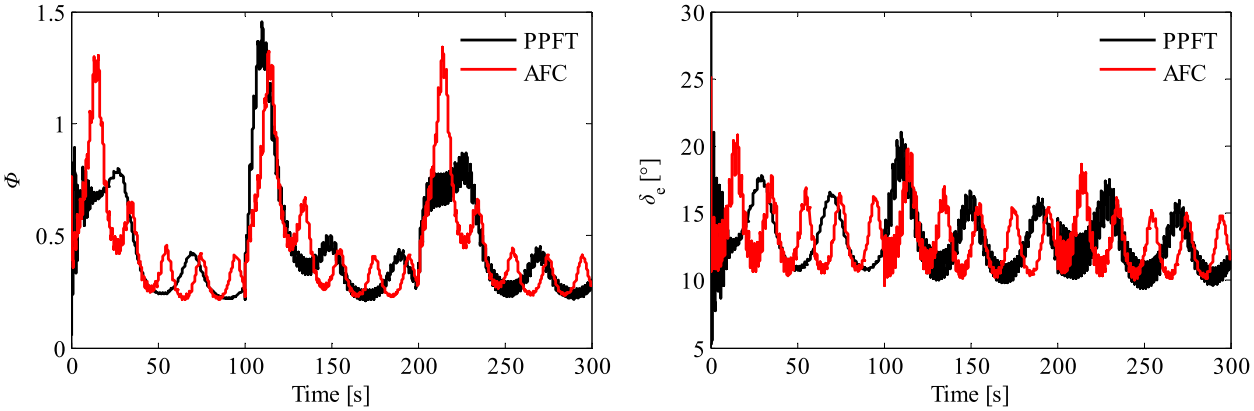

FIGURE 15. Control inputs.

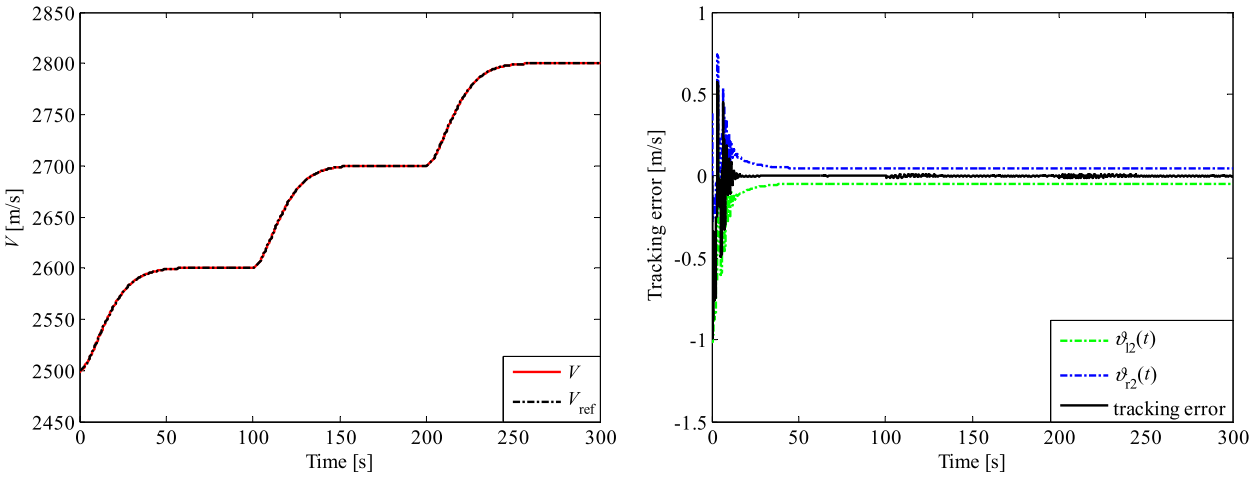

FIGURE 16. Velocity tracking performance.

functions of the altitude subsystem and the velocity subsystem are $(1-0.05\sin(Q))\,\delta_e$ and $(1-0.1\sin(V))\,\Phi$ respectively. The simulation time is set to 80s. The external disturbance functions $d_0(t) = 0.04\sin(0.5\pi t)$ and $d_{V0}(t) = 2\sin(0.1\pi t)$ occur at 30s. In order to verify the superiority of the control method (PPFT) proposed in this paper, the simulation results are compared with the following two methods. One is observer-based fault-tolerant (OFT) control method in [51] and the other is the neural adaptive control (NAC) control method in [45].

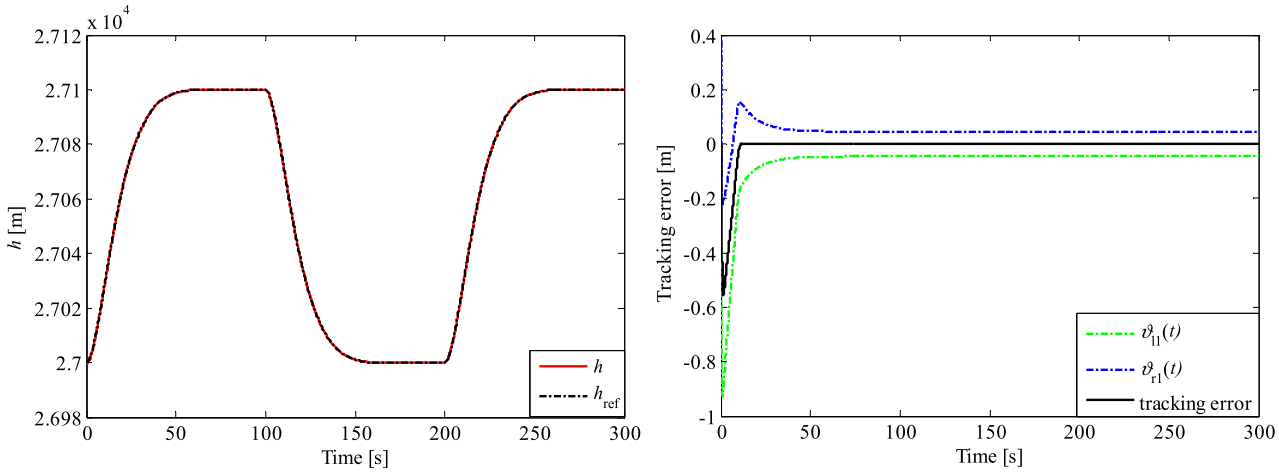

FIGURE 17. Altitude tracking performance.

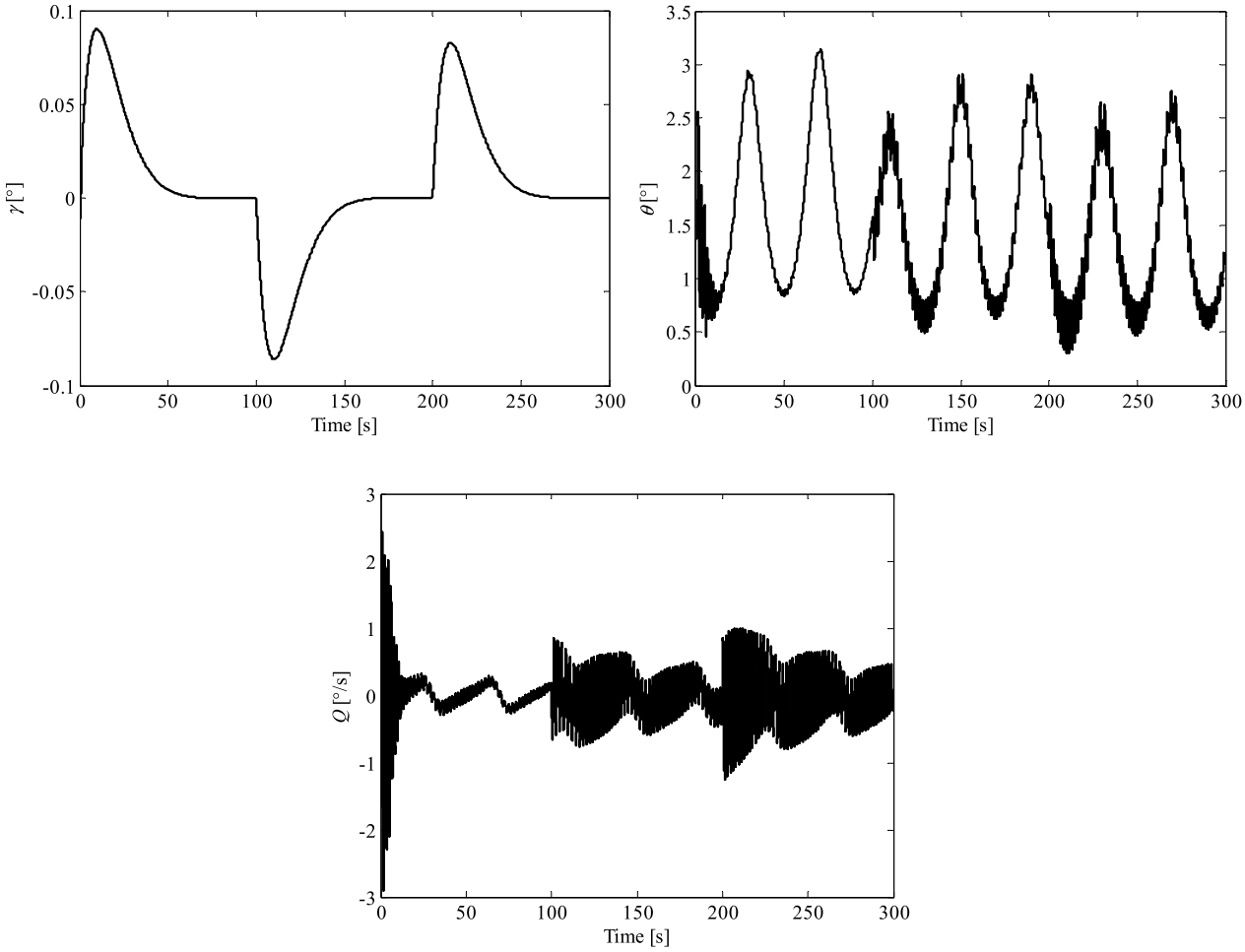

FIGURE 18. Altitude angles.

The simulation results compared with OFT and NAC are shown from Fig. 4 to Fig. 10. In Fig. 4, the velocity and altitude of OFT and NAC tracking performance significantly decreased after adding disturbance functions, but PPFT method keeps better tracking performance. In Fig. 5 and 6, the tracking errors of both OFT and NAC methods are significantly larger than those of PPFT method, and the tracking errors of PPFT method can maintain the

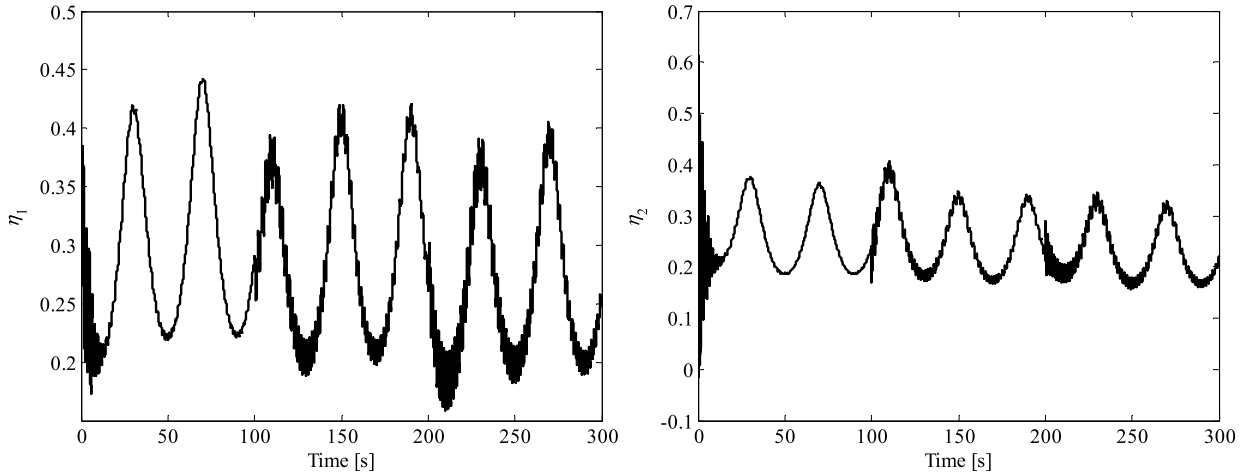

FIGURE 19. Flexible states.

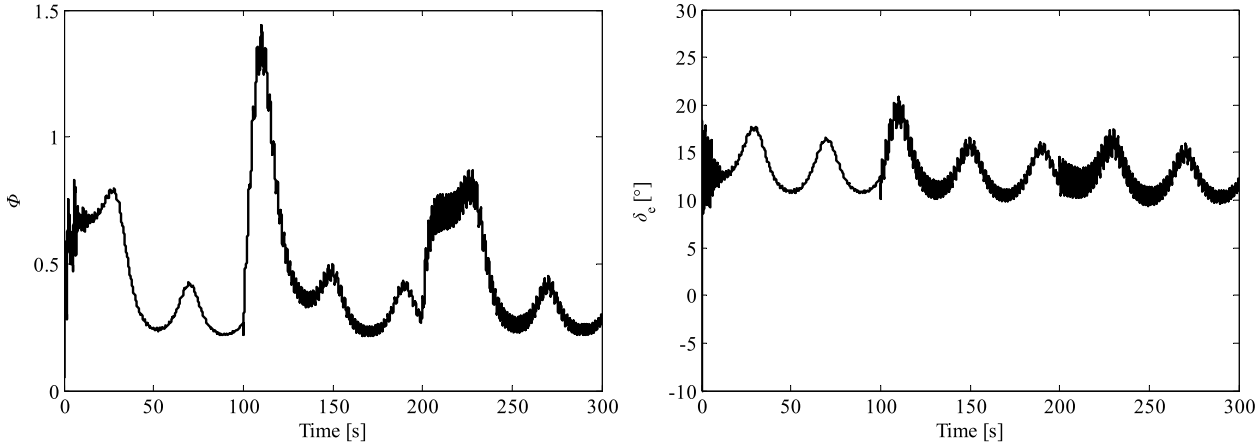

FIGURE 20. Control inputs.

prescribed transient performance and steady-state accuracy. For control inputs and flexible states, although the three methods are smoother and there is no high frequency buffeting. The buffetings of OFT and NAC are significantly stronger than that of PPFT. Two transform error functions are bounded in Fig. 10. Actually, the NAC and OFT methods have been able to ensure high steady state performance of HFV, especially since the error accuracy of the NAC method is small enough. However, the PPFT method can not only guarantee better steady-state performance of tracking errors than the previous two methods, but also guarantee satisfactory transient performance of tracking errors. The PPFT method has more energy consumption than the previous two methods while achieving small computation load and satisfactory control performance.

Meanwhile, the PPFT method in this paper is compared with that in [52] (actuator failure compensation control, AFC) without disturbance. In the simulation experiment, V_c is a step signal that increments by 100m/s every 100s and h_c is a square wave signal with the period of 200s and amplitude of 100m. The simulation time is set to 300s.

The simulation results are shown in Fig. 11 to Fig. 15. The Fig. 11 shows that PPFT method has better velocity tracking performance in both steady-state accuracy and transient performance. Although in Fig. 12, the altitude error's overshoot and stability time of PPFT method are a little worse than those of AFC method. However, the steady state accuracy of PPFT method is higher. Furthermore, although there is no high frequency buffeting in the altitude angle response and flexible states of the two methods, it can still be seen from the Figs. 13 and 14 that the buffeting amplitude of the PPFT method is smaller and more stable. Fig. 15 indicates that the responses of control inputs are satisfactory. It can be said that the PPFT method achieves more stable HFV flight control while sacrificing some transient performance.

In order to further illustrate the effectiveness of the proposed method, the initial values of HFV model are partially changed and the simulation experiment is carried out. The initial values of the modified HFV model are shown in Tab. 3. Simulation results are shown in Fig. 16 to Fig. 20. Although only the initial values of HFV model are changed slightly, it can be clearly seen that the initial value of tracking errors

TABLE 3. HFV initial valueS after the change.

State	Value
V	2500m/s
h	27000 m
γ	0 deg
θ	1.6301 deg
$\mathcal{Q}$	0 deg/s
η_1	0.2692
η_2	0.2402

become negative. However, the tracking performance is still satisfied. Meanwhile, the initial values of the tracking error are either positive or negative, which indicate the effectiveness of the method.

V. CONCLUSION

In this paper, a novel prescribed performance fault tolerant control for HFV nonaffine model with actuator failures is proposed. Based on timescale principle, the HFV model is decomposed into two subsystems: the altitude subsystem and the velocity subsystem, which are expressed in nonaffine forms to design the controller. In order to achieve satisfactory transient performance and steady-state accuracy of tracking error, a new performance function is designed. The function satisfies small overshoot of tracking error and the boundary of performance function varies with tracking error adaptively. For the altitude subsystem, the simplified step backstepping control with actuator failures is proposed which reduces the computational load. A prescribed performance fault-tolerant control law is also designed for the velocity subsystem with actuator failures. The Lyapunov functional is used to prove the boundedness of all the signals in closed-loop system. Through simulation experiments, the proposed method is compared with three existing control methods. The method proposed in this paper can provide better robust tracking performance of velocity and altitude reference inputs while guaranteeing satisfactory transient and steady-state accuracy. Furthermore, after changing the initial value of the system, the control method can still ensure satisfactory tracking performance, which further proves the effectiveness of the method. The method proposed in this paper has certain engineering application significance, which can lay a foundation for the subsequent research on the prescribed performance fault tolerant control of HFV non-affine model. Furthermore, the model failure types considered in this paper are complete and closer to the actual situation, which can lay a foundation for a complete fault-tolerant detection and control mechanism in the future.

ACKNOWLEDGMENT

Siyuan Zhao thanks Dr. Xiangwei Bu for his fund support.

REFERENCES

[1] C.-Y. Sun, C.-X. Mu, and Y. Yu, "Some control problems for near space hypersonic vehicles," *Acta Autom. Sinica*, vol. 39, no. 11, pp. 1901–1913, Nov. 2013.
[2] E. A. Morelli, "Flight-test experiment design for characterizing stability and control of hypersonic vehicles," *J. Guid., Control, Dyn.*, vol. 32, no. 3, pp. 949–959, May/Jun. 2009.
[3] B. Xu and Z.-K. Shi, "An overview on flight dynamics and control approaches for hypersonic vehicles," *Sci. China Inf. Sci.*, vol. 58, no. 7, pp. 1–19, Jul. 2015.
[4] R. T. Voland, L. D. Huebner, and C. R. McClinton, "X-43A hypersonic vehicle technology development," *Acta Astron.*, vol. 59, nos. 1–5, pp. 181–191, Jul./Sep. 2006.
[5] J. Hank, J. Murphy, and R. Mutzman, "The X-51A scramjet engine flight demonstration program," in *Proc. 15th AIAA Int. Space Planes Hypersonic Syst. Technol. Conf.*, Dayton, OH, USA, Apr. 2008, p. 2540.
[6] J. J. Bertin and R. M. Cummings, "Fifty years of hypersonics: Where we've been, where we're going," *Prog. Aerosp. Sci.*, vol. 39, nos. 6–7, pp. 511–536, Aug./Oct. 2003.
[7] O. A. Powell, J. T. Edwards, R. B. Norris, K. E. Numbers, and J. A. Pearce, "Development of hydrocarbon-fueled scramjet engines: The hypersonic technology (HyTech) program," *J. Propuls. Power*, vol. 17, no. 6, pp. 1170–1176, Nov./Dec. 2001.
[8] D. Preller and M. K. Smart, "Longitudinal control strategy for hypersonic accelerating vehicles," *J. Spacecraft Rockets*, vol. 52, no. 3, pp. 993–998, May/Jun. 2015.
[9] E. T. Curran, "Scramjet engines: The first forty years," *J. Propuls. Power*, vol. 17, no. 6, pp. 1138–1148, Nov./Dec. 2001.
[10] J. Li, S. Chen, C. Li, C. Gao, and W. Jing, "Adaptive control of underactuated flight vehicles with moving mass," *Aerosp. Sci. Technol.*, vol. 85, pp. 75–84, Feb. 2019.
[11] J. Q. Li, C. Gao, C. Li, and W. Jing, "A survey on moving mass control technology," *Aerosp. Sci. Technol.*, vol. 82, pp. 594–606, Nov. 2018.
[12] G. Ma, C. Chen, Y. Lyu, and Y. Guo, "Adaptive backstepping-based neural network control for hypersonic reentry vehicle with input constraints," *IEEE Access*, vol. 6, pp. 1954–1966, 2017.
[13] D. Zhang, S. Tang, L. Cao, F. Cheng, and F. Deng, "Research on control-oriented coupling modeling for air-breathing hypersonic propulsion systems," *Aerosp. Sci. Technol.*, vol. 84, pp. 143–157, Jan. 2019.
[14] D. Xiao, M. Liu, Y. Liu, and Y. Lu, "Switching control of a hypersonic vehicle based on guardian maps," *Acta Astronautica*, vol. 122, pp. 294–306, May/Jun. 2016.
[15] J. Song, L. Wang, G. Cai, and X. Qi, "Nonlinear fractional order proportion-integral-derivative active disturbance rejection control method design for hypersonic vehicle attitude control," *Acta Astronautica*, vol. 111, pp. 160–169, Jun./Jul. 2015.
[16] Y. Chang, T. Jiang, and Z. Pu, "Adaptive control of hypersonic vehicles based on characteristic models with fuzzy neural network estimators," *Aerosp. Sci. Technol.*, vol. 68, pp. 475–485, Jun. 2017.
[17] L. Q. Dou, J. Gao, Q. Zong, and Z. Ding, "Modeling and switching control of air-breathing hypersonic vehicle with variable geometry inlet," *J. Franklin Inst.*, vol. 355, no. 15, pp. 6904–6926, Oct. 2018.
[18] X. Bu, X. Wu, R. Zhang, Z. Ma, and J. Huang, "Tracking differentiator design for the robust backstepping control of a flexible air-breathing hypersonic vehicle," *J. Franklin Inst.*, vol. 352, no. 4, pp. 1739–1765, Apr. 2015.
[19] B. Xu and Y. Zhang, "Neural discrete back-stepping control of hypersonic flight vehicle with equivalent prediction model," *Neurocomputing*, vol. 154, pp. 337–346, Apr. 2015.
[20] D. Gao, S. Wang, and H. Zhang, "A singularly perturbed system approach to adaptive neural back-stepping control design of hypersonic vehicles," *J. Intell. Robot. Syst.*, vol. 73, nos. 1–4, pp. 249–259, Jan. 2014.
[21] J. Wang, Y. Wu, and X. Dong, "Recursive terminal sliding mode control for hypersonic flight vehicle with sliding mode disturbance observer," *Nonlinear Dyn.*, vol. 81, no. 3, pp. 1489–1510, Aug. 2015.
[22] Y. Zhang and B. Xian, "Continuous nonlinear asymptotic tracking control of an air-breathing hypersonic vehicle with flexible structural dynamics and external disturbances," *Nonlinear Dyn.*, vol. 83, nos. 1–2, pp. 867–891, Jan. 2016.
[23] R. Zhang, C. Sun, J. Zhang, and Y. Zhou, "Second-order terminal sliding mode control for hypersonic vehicle in cruising flight with sliding mode disturbance observer," *J. Control Theory Appl.*, vol. 11, no. 2, pp. 299–305, May 2013.

[24] S. Zhang, Q. Wang, G. Yang, and M. Zhang, "Anti-disturbance backstepping control for air-breathing hypersonic vehicles based on extended state observer," *ISA Trans.*, to be published. doi: 10.1016/j.isatra.2019.02.017.
[25] Y. Xu, B. Jiang, G. Tao, and Z. Gao, "Fault accommodation for near space hypersonic vehicle with actuator fault," *Int. J. Innov. Comput., Inf. Control*, vol. 7, no. 5, pp. 2187–2200, May 2011.
[26] B. Jiang, D. Xu, P. Shi, and C. C. Lim, "Adaptive neural observer-based backstepping fault tolerant control for near space vehicle under control effector damage," *IET Control Theory Appl.*, vol. 8, no. 9, pp. 658–666, 2014.
[27] B. Jiang, Z. Gao, P. Shi, and Y. Xu, "Adaptive fault-tolerant tracking control of near-space vehicle using Takagi–Sugeno fuzzy models," *IEEE Trans. Fuzzy Syst.*, vol. 18, no. 5, pp. 1000–1007, Oct. 2010.
[28] X. Hu, H.-R. Karimi, L. Wu, and Y. Guo, "Model predictive control-based non-linear fault tolerant control for air-breathing hypersonic vehicles," *IET Control Theory Appl.*, vol. 8, no. 13, pp. 1147–1153, Sep. 2014.
[29] C. P. Bechlioulis and G. A. Rovithakis, "Robust adaptive control of feedback linearizable MIMO nonlinear systems with prescribed performance," *IEEE Trans. Autom. Control*, vol. 53, no. 9, pp. 2090–2099, Oct. 2008.
[30] C. P. Bechlioulis and G. A. Rovithakis, "A low-complexity global approximation-free control scheme with prescribed performance for unknown pure feedback systems," *Automatica*, vol. 50, no. 4, pp. 1217–1226, Apr. 2014.
[31] Y. Wang, J. Hu, J. Wang, and X. Xing, "Adaptive neural novel prescribed performance control for non-affine pure-feedback systems with input saturation," *Nonlinear Dyn.*, vol. 93, no. 3, pp. 1241–1259, Aug. 2018.
[32] C. Wei, J. Luo, H. Dai, Z. Bian, and J. Yuan, "Learning-based adaptive prescribed performance control of postcapture space robot-target combination without inertia identifications," *Acta Astronautica*, vol. 146, pp. 228–242, May 2018.
[33] H. Song, T. Zhang, G. Zhang, and C. Lu, "Robust dynamic surface control of nonlinear systems with prescribed performance," *Nonlinear Dyn.*, vol. 76, no. 1, pp. 599–608, Apr. 2014.
[34] B. Fu, K. Chen, and H. Guo, "Second-order sliding mode disturbance observer-based adaptive fuzzy tracking control for near-space vehicles with prescribed tracking performance," *Mathematical Problems Eng.*, vol. 2018, May 2018, Art. no. 4253971. doi: 10.1155/2018/4253971.
[35] G. Zhu and J. Liu, "Neural network-based adaptive backstepping control for hypersonic flight vehicles with prescribed tracking performance," *Math. Problems Eng.*, vol. 2015, Apr. 2015, Art. no. 591789. doi: 10.1155/2015/591789.
[36] H.-W. Zhao and Y. Liang, "Prescribed performance dynamic neural network control for a flexible hypersonic vehicle with unknown control directions," *Adv. Mech. Eng.*, vol. 11, no. 4, Apr. 2019, Art. no. 1687814019841489.
[37] M. A. Bolender and D. B. Doman, "Nonlinear longitudinal dynamical model of an air-breathing hypersonic vehicle," *J. Spacecraft Rockets*, vol. 44, no. 2, pp. 374–387, 2007.
[38] J. T. Parker, A. Serrani, S. Yurkovich, M. A. Bolender, and D. B. Doman, "Control-oriented modeling of an air-breathing hypersonic vehicle," *J. Guid., Control, Dyn.*, vol. 30, no. 3, pp. 856–869, 2007.
[39] Z. D. Wilcox, W. MacKunis, S. Bhat, R. Lind, and W. E. Dixon, "Lyapunov-based exponential tracking control of a hypersonic aircraft with aerothermoelastic effects," *J. Guid. Control Dyn.*, vol. 33, no. 4, pp. 1213–1224, Jul. 2010.
[40] S. I. Han and J. M. Lee, "Fuzzy echo state neural networks and funnel dynamic surface control for prescribed performance of a nonlinear dynamic system," *IEEE Trans. Ind. Electron.*, vol. 61, no. 2, pp. 1099–1112, Feb. 2014.
[41] E. J. Hartman, J. D. Keeler, and J. M. Kowalski, "Layered neural networks with Gaussian hidden units as universal approximations," *Neural Comput.*, vol. 2, no. 2, pp. 210–215, Jun. 1990.
[42] J. Park and I. W. Sandberg, "Universal approximation using radial-basis function networks," *Neural Comput.*, vol. 3, no. 2, pp. 246–257, 1991.
[43] C. Wei, J. Luo, Z. Yin, and J. Yuan, "Leader-following consensus of second-order multi-agent systems with arbitrarily appointed-time prescribed performance," *IET Control Theory Appl.*, vol. 12, no. 16, pp. 2276–2286, Nov. 2018.
[44] B. Xu, "Robust adaptive neural control of flexible hypersonic flight vehicle with dead-zone input nonlinearity," *Nonlinear Dyn.*, vol. 80, no. 3, pp. 1509–1520, 2015.
[45] W. Fu, Y. Wang, S. Zhu, and Y. Xia, "Neural adaptive control of hypersonic aircraft with actuator fault using randomly assigned nodes," *Neurocomputing*, vol. 174, pp. 1070–1076, Jan. 2016.
[46] Z. Yin, J. Luo, and C. Wei, "Quasi fixed-time fault-tolerant control for nonlinear mechanical systems with enhanced performance," *Appl. Math. Comput.*, vol. 352, pp. 157–173, Jul. 2019.
[47] J. He, R. Qi, B. Jiang, and J. Qian, "Adaptive output feedback fault-tolerant control design for hypersonic flight vehicles," *J. Franklin Inst.*, vol. 352, no. 5, pp. 1811–1835, 2015.
[48] X. Bu, G. He, and D. Wei, "A new prescribed performance control approach for uncertain nonlinear dynamic systems via back-stepping," *J. Franklin Inst.*, vol. 355, no. 17, pp. 8510–8536, Nov. 2018.
[49] Y. Wang and J. Hu, "Improved prescribed performance control for air-breathing hypersonic vehicles with unknown deadzone input nonlinearity," *ISA Trans.*, vol. 79, pp. 95–107, Aug. 2018.
[50] H. Gao and Y. Cai, "Nonlinear disturbance observer-based model predictive control for a generic hypersonic vehicle," *Proc. Inst. Mech. Eng., I, J. Syst. Control Eng.*, vol. 230, no. 1, pp. 3–12, Jan. 2016.
[51] G. Gao and J. Wang, "Observer-based fault-tolerant control for an air-breathing hypersonic vehicle model," *Nonlinear Dyn.*, vol. 76, no. 1, pp. 409–430, 2014.
[52] W. Wang and C. Wen, "Adaptive actuator failure compensation control of uncertain nonlinear systems with guaranteed transient performance," *Automatica*, vol. 46, no. 12, pp. 2082–2091, 2010.

SIYUAN ZHAO received the B.S. degree in measurement and control engineering from Air Force Engineering University, in 2013, where he is currently pursuing the M.S. degree in control science and engineering. He was involved in the guidance and the control method of hypersonic vehicles.

XIAOBING LI received the B.S. degree in aircraft guidance and control from Northwestern Polytechnical University, in 1988, and the M.S. degree in control science and engineering from Air Force Engineering University, in 1991, where he is currently a Professor of control science and engineering. His research interests include the control theory and aircraft control, and guidance and navigation.